

# CHAPTER-III

## EXPERIMENTAL SECTION

### III.1. NAME, STRUCTURE, PHYSICAL AND CHEMICAL PROPERTIES, PURIFICATION AND APPLICATIONS OF THE CHEMICALS USED IN THE RESEARCH WORK

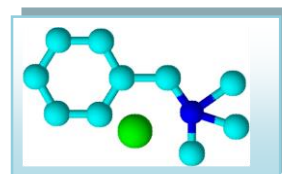
#### III.1.1 Ionic Liquids

➤ ***Benzyltrimethylammonium chloride:***

*Benzyltrimethylammonium chloride* is a light yellow solid with a mild almond odor, exists as a molten solid phase (white crystalline) with the melting point 243°C.

- ❖ **Source:** Sigma Aldrich, Germany
- ❖ **Purification:** Used as purchased. The purity of the chemical is >99.0%
- ❖ **Application:**

*Benzyltrimethylammonium chloride* used as plating agents and surface treating agents, processing aids, not otherwise listed, surface active agents, Electrical and Electronic Products, Fabric, Textile, and Leather Products not covered elsewhere, Paints and Coatings



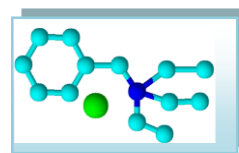
<b><i>Benzyltrimethylammonium chloride</i></b>	
<i>Appearance</i>	: White Crystalline
<i>Molecular Formula</i>	: $C_{10}H_{16}ClN$
<i>Molecular Weight</i>	: $185.695g \cdot mol^{-1}$
<i>Melting Point</i>	: $243^{\circ}C$
<i>Relative Density</i>	: 1.07

➤ ***Benzyltriethylammonium chloride:***

*Benzyltrimethylammonium chloride*, is a quaternary ammonium salt that functions as an organic base. It is usually handled as a solution in water or methanol. The compound is colourless though the solutions often appear slightly yellowish. Commercial samples often have a distinctive fish-like odor, presumably due to the presence of trimethylamine via hydrolysis.

- ❖ **Source:** Sigma Aldrich, Germany
- ❖ **Purification:** Used as purchased. The purity of the chemical is >99.0%
- ❖ **Application:**

*Benzyltriethylammonium chloride* is perhaps used as phase transfer catalyst. The ionic liquid may be used in organic synthesis and bio-catalysis, dye sensitized-cells, batteries, electrochemical application and phase transfer catalyst, etc.



***Benzyltriethylammonium  
chloride***

<i>Appearance</i>	: <i>White Crystalline</i>
<i>Molecular Formula</i>	: $C_{13}H_{22}ClN$
<i>Molecular Weight</i>	: $227.776 \text{ g}\cdot\text{mol}^{-1}$
<i>Relative Density</i>	: <i>No data available</i>

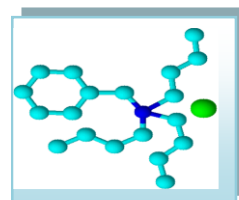
➤ ***Benzyltributylammonium chloride:***

*Benzyltributylammonium chlorides* are quaternary ammonium compounds. They have a central nitrogen atom which is joined to four organic radicals and one acid radical. They are prepared by treatment of an amine with an alkylating agent. They show a variety of physical, chemical, and biological properties and most compounds are soluble in water and strong electrolytes.

- ❖ **Source:** Sigma Aldrich, Germany
- ❖ **Purification:** Used as purchased. The purity of the chemical is >98.0%

❖ **Application:**

The ionic liquid Benzyltributylammonium chloride used for synthesis, antistatic Agent, detergent sanitisers, softner for textiles and paper products, phase transfer catalyst, antimicrobials, disinfection agents And sanitizers, Slimicidal Agents, Algaecide, Emulsifying Agents, Pigment Dispersers



***Benzyltributylammonium  
chloride***

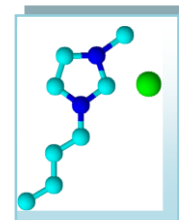
<i>Appearance</i>	: <i>White Crystalline</i>
<i>Molecular Formula</i>	: $C_{19}H_{34}ClN$
<i>Molecular Weight</i>	: $311.938 \text{ g}\cdot\text{mol}^{-1}$
<i>Melting point</i>	: $152-159 \text{ C}$

➤ **1-butyl-3-methylimidazolium chloride:**

1-butyl-3-methylimidazolium chloride anionic liquid based on imidazole chemistry.

- ❖ **Source:** Sigma Aldrich, Germany
- ❖ **Purification:** Used as purchased. The purity of the chemical is >99.0%
- ❖ **Application:**

1-butyl-3-methylimidazolium chloride is currently of interest in industry due to their ability to be infinitely recycled and their amenability to solvation at room temperature, making them excellent green solvents.



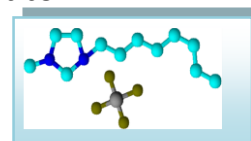
<b>1-butyl-3-methylimidazolium chloride</b>	
<i>Appearance</i>	: White Crystalline
<i>Molecular Formula</i>	: $C_8H_{15}ClN_2$
<i>Molecular Weight</i>	: $174.67 \text{ g}\cdot\text{mol}^{-1}$
<i>Relative Density</i>	: No data available

➤ **1-methyl-3-octylimidazolium tetrafluoroborate:**

1-methyl-3-octylimidazolium tetrafluoroborate is an imidazolium based ionic liquid, of molecular formula  $C_{12}H_{23}BF_4N_2$ , containing methyl, octyl group with two active nitrogen atoms in the imidazole or five member ring, exist as a molten liquid phase.

- ❖ **Source:** Sigma Aldrich, Germany
- ❖ **Purification:** Used as purchased. The purity of the chemical is >99.0%
- ❖ **Application:**

1-methyl-3-octylimidazolium tetrafluoroborate is used as solvents for polymer chemistry. The ionic liquid are good examples of neoteric solvents, new types of solvents, or older materials that are finding new applications as solvents, which is environmentally friendly (or eco-friendly) because they are less hazardous for human body as well as less toxic for living organisms, used as recyclable solvents for organic reactions and



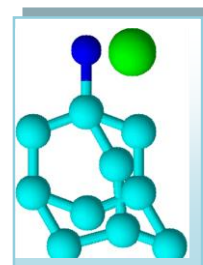
<b>1-methyl-3-octylimidazolium tetrafluoroborate</b>	
<i>Appearance</i>	: liquid
<i>Molecular Formula</i>	: $C_{12}H_{23}BF_4N_2$
<i>Molecular Weight</i>	: $282.13 \text{ g}\cdot\text{mol}^{-1}$
<i>Relative Density</i>	: $1.1070 \text{ g}\cdot\text{cm}^{-3}$

separation processes, lubricating fluids, heat transfer fluids for processing biomass and electrically conductive liquids as electrochemical device in the field of electrochemistry (batteries and solar cells) and so forth. In the modern technology, industry, and also in academic research field, the vast application is frequently increases.

### III.1. 2 Drug Molecules

#### ➤ **Amantadine Hydrochloride:**

Amantadine is an antiviral and an antiparkinsonian drug. This drug has U.S. Food and Drug Administration approval. 1-adamantylamine or 1-aminoadamantane contains an adamantane backbone that has an amino group which is substituted at one of the four methyne positions. One derivative of adamantane is rimantadine which has parallel biological properties.



<b>Amantadine Hydrochloride</b>	
<i>Appearance</i>	: white crystalline solid
<i>Molecular Formula</i>	: $C_{10}H_{18}NCl$
<i>Molecular Weight</i>	: $151.249 \text{ g}\cdot\text{mol}^{-1}$
<i>Melting Point</i>	: $273.15 \text{ K}$
<i>Relative Density</i>	: $1.247 \text{ g}\cdot\text{cm}^{-3}$

❖ **Source:** Sigma Aldrich, Germany

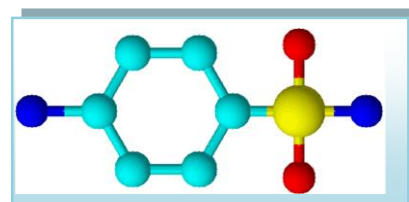
❖ **Purification:** Used as purchased. The chemical more than 95.0% pure.

❖ **Application:**

Apart from medical uses, this compound is useful as a building block in organic synthesis, allowing the insertion of an adamantyl group.

#### ➤ **Sulphanilamide:**

Sulphanilamide (also spelled sulphanilamide) is a sulfonamide antibacterial. Chemically, it is an organic compound consisting of an aniline derivatized with a sulfonamide group.



<b>Sulphanilamide</b>	
<i>Appearance</i>	: Crystalline
<i>Molecular Formula</i>	: $C_6H_8N_2O_2S$
<i>Molecular Weight</i>	: $172.80 \text{ g}\cdot\text{mol}^{-1}$
<i>Melting Point</i>	: $165 \text{ C}$
<i>Relative Density</i>	: $1.08 \text{ g}\cdot\text{cm}^{-3}$

❖ **Source:** Sigma Aldrich, Germany

❖ **Purification:** Used as purchased. The purity of the chemical is >98.0%

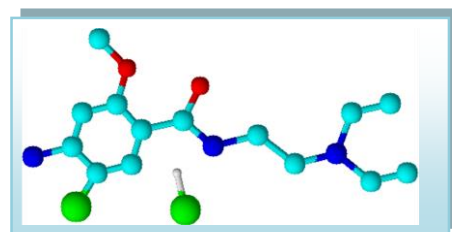
❖ **Application:**

In the World War II to Powdered sulfanilamide was used to reduce infection rates, which helped widely to reduce the mortality rate than earlier wars. Modern antibiotics are associated with supplanted sulfanilamide; however, sulfanilamide remains in use for treatment of vaginal yeast infections.

➤ **Metoclopramide Hydrochloride:**

Metoclopramide hydrochloride (MP) is a white crystalline, odorless substance, freely soluble in water. Chemically, it is 4-amino-5-chloro-N-[2-(diethylamino) ethyl]-2-methoxy benzamide monohydrochloride.

- ❖ **Source:** Sigma Aldrich, Germany
- ❖ **Purification:** Used as purchased. The purity of the chemical is >98.0%
- ❖ **Application:**



<b>Metoclopramide Hydrochloride</b>	
<i>Appearance</i>	:Crystalline
<i>Molecular Formula</i>	:C <sub>14</sub> H <sub>23</sub> Cl <sub>2</sub> N <sub>3</sub> O <sub>2</sub>
<i>Molecular Weight</i>	:299.80 g·mol <sup>-1</sup>
<i>Melting Point</i>	: 147.3 C
<i>Relative Density</i>	:1.08 g·cm <sup>-3</sup>

Metoclopramide hydrochloride (MP) is used as an anti-emetic in the treatment of some forms of nausea and vomiting and to treat heartburn caused by gastroesophageal reflux in people who have used other medications without relief of symptoms. MP have a greater impact on the treatment of disorders of the gastrointestinal tract. MP is prokinetic agents in gastroenterology. Prokinetic drugs enhances the response to acetylcholine of tissue in upper gastrointestinal tract causing enhanced motility and accelerated gastric emptying without stimulating gastric, biliary, or pancreatic secretions; increases lower oesophageal sphincter tone.

### III.1.3 Macrocyclic Compounds

➤ **α-Cyclodextrin (α-CD) :**

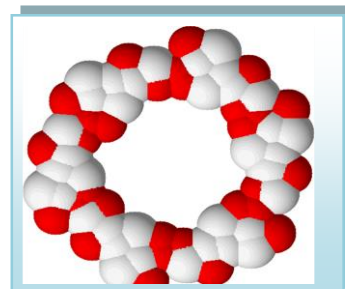
**α-Cyclodextrin** is a cyclic oligosaccharide composed of 6 glucose groups. This is white amorphous solid having a cylinder like molecular structure. The structural

arrangement makes it versatile in different fields. The properties are widely used in industry for various purpose.

- ❖ **Source:** Sigma Aldrich, Germany.
- ❖ **Purification:** Used as purchased. The purity is 99.98%.

❖ **Application:**

$\alpha$ -Cyclodextrin is a new substance which can be widely applied in production and modification of medicine, food, amino acids, vitamins and many essential substrates for animals. It can be applied widely in improving stability, solubility and good odour. In the production of medicine, it can strengthen the stability of medicine without being oxidized and resolving. On the other hand, it can improve the solubility incorporating the drug molecule inside into it. Due to its proper cavity size it is very useful in Host-Guest chemistry. It can also be used to lower the toxicity and side-effect of medicine and cover the strange and bad smell. It again improves the stability of perfume and condiment and keeps food dry or wet at will.  $\beta$ -CD with a cavity diameter of 4.7-5.3 Å, is of great interest because its cavity size allows for a number of substrates to fit inside it. Like other host molecules e.g.,  $\gamma$ -cyclodextrin, calixarin, cucarbit etc. it can accommodate small molecules as guest molecules. For this reason,  $\alpha$ -cyclodextrin is widely used as a complexing agent with hormones, vitamins, and many compounds and these are frequently used in tissue and cell culture applications. Thus  $\alpha$ -cyclodextrin plays a vital role in the host-guest chemistry and its low cost production helps it to be versatile.

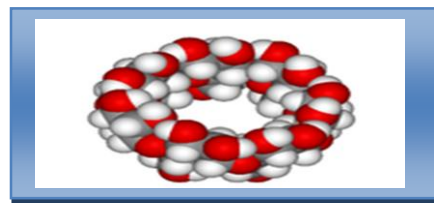


**$\alpha$ -Cyclodextrin**

<i>Appearance</i>	:Crystalline Powder
<i>Molecular Formula</i>	$C_{42}H_{70}O_{35}$
<i>Molecular Weight</i>	:1134.98 $g \cdot mol^{-1}$
<i>Melting Point</i>	:563.15-573.15 K
<i>Boiling Point</i>	:1814.33 K
<i>Relative Density</i>	:1.44 $g \cdot cm^{-3}$ at 20°C
<i>Refractive Index</i>	:1.59 ( $n_D^{20}$ )

➤  **$\beta$ -Cyclodextrin ( $\beta$ -CD):**

**$\beta$ -Cyclodextrin** is white amorphous solid compound composed of 7 glucose groups having a cylinder like molecular structure. The function of  $\beta$ -Cyclodextrin depends on its molecular structure which can be easy to integrate other materials. That feature is applied widely in industry.



- ❖ **Source:** Sigma Aldrich, Germany.
- ❖ **Purification:** Used as purchased. The purity is 99.98%.
- ❖ **Application:**

<b><math>\beta</math>-Cyclodextrin</b>	
<i>Appearance</i>	:Crystalline Powder
<i>Molecular Formula</i>	: $C_{42}H_{70}O_{35}$
<i>Molecular Weight</i>	:1134.98 $g \cdot mol^{-1}$
<i>Melting Point</i>	:563.15-573.15 K
<i>Boiling Point</i>	:1814.33 K
<i>Relative Density</i>	:1.44 $g \cdot cm^{-3}$ at 20°C
<i>Refractive Index</i>	:1.59 ( $n_D^{20}$ )

$\beta$ -Cyclodextrin is a new stuff which can be widely applied in production of medicine and food. It can be applied widely in production of medicine, food and cosmetics, whose function is improved stability, solubility and good smelled. In the production of medicine, it can strengthen the stability of medicine without being oxidized and resolving. On the other hand, it can improve the solubility. And the effect on living of medicine, lower the toxic and side-effect of medicine and cover the strange and bad smell. In the production of food, it can mainly cover strange and bad smell of food, improve the stability of perfume and condiment and keep food dry or wet at will.  $\beta$ -CD with a cavity diameter of 6.4-7.5 Å, is the most interest because its cavity size allows for the best special fit for many common guest moieties. For this reason,  $\beta$ -cyclodextrin is most commonly used as a complexing agent in hormones, vitamins, and many compounds frequently used in tissue and cell culture applications. This capability has also been of assistance for different applications in medicines, cosmetics, food technology, pharmaceutical, and chemical industries as well as in agriculture and environmental engineering as an encapsulating agent to protect sensitive molecules in hostile environment.

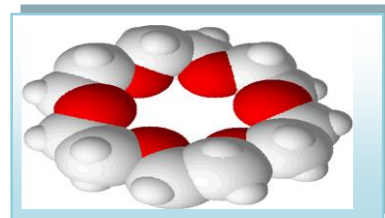
➤ **18-crown-6:**

1,4,7,10,13,16-hexaoxacyclooctadecane in short 18-Crown-6 has a molecular structure  $[C_{12}H_{24}O_6]$ . It is a white, hygroscopic crystalline solid with a low melting point.

- ❖ **Source:** Sigma Aldrich, Germany
- ❖ **Purification:** Used as purchased. The purity of the chemical is >98.0%
- ❖ **Application:**

18-Crown-6 binds to a variety of small cations, using all six oxygens as donor atoms.

Crown ethers are often used as phase transfer catalysts. For example, potassium permanganate dissolves in benzene in the presence of 18-crown-6, giving the so-called "purple benzene", which can be used to oxidize diverse organic compounds.



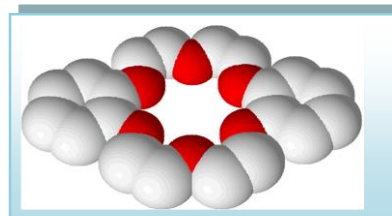
<b>18-crown-6</b>	
<i>Appearance</i>	:Crystalline
<i>Molecular Formula</i>	: $C_{12}H_{24}O_6$
<i>Molecular Weight</i>	: $264.315 \text{ g}\cdot\text{mol}^{-1}$
<i>Melting Point</i>	: 37 to 40 C
<i>Relative Density</i>	: $1.237 \text{ g}\cdot\text{cm}^{-3}$

➤ **Dibenzo-18-crown-6:**

Dibenzo-18-Crown-6 has strong complexing abilities and has high affinity for alkali metal cations.

- ❖ **Source:** Sigma Aldrich, Germany
- ❖ **Purification:** Used as purchased. The purity of the chemical is >98.0%
- ❖ **Application:**

Dibenzo-18-Crown-6 can be used as phase transfer catalysts for monoazaporphyrin syntheses and also used for ion transfer across membranes and as a synthon for preparation of liquid crystal polyesters.



<b>Dibenzo-18-crown-6</b>	
<i>Appearance</i>	:hygroscopic crystalline solid
<i>Molecular Formula</i>	: $C_{20}H_{24}O_6$
<i>Molecular Weight</i>	: $360.41 \text{ g}\cdot\text{mol}^{-1}$

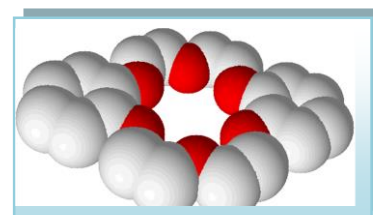


➤ **Dicyclo-18-crown-6:**

Dicyclo-18-Crown-6 has strong complexing abilities and has high affinity for alkali metal cations.

- ❖ **Source:** Sigma Aldrich, Germany
- ❖ **Purification:** Used as purchased. The purity of the chemical is >98.0%
- ❖ **Application:**

Dicyclo-18-Crown-6 can be used as phase transfer catalysts and also used for ion transfer across membranes.



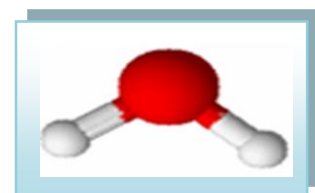
<b>Dicyclo-18-crown-6</b>	
<i>Appearance</i>	:hygroscopic crystalline solid
<i>Molecular Formula</i>	: $C_{20}H_{36}O_6$
<i>Molecular Weight</i>	:372.496 $g \cdot mol^{-1}$

### III.1.4 Solvents

The details of the aqueous and non-aqueous solvents used in the research work are given below:

➤ **Water ( $H_2O$ ):**

Water is an omnipresent chemical substance is composed of hydrogen and oxygen and is essential for all known forms of life. In typical usage, water refers only to its liquid form or state, but the substance also exists as solid state, ice, and a gaseous state, water vapour or steam. Water is a good solvent and is often referred to as the universal solvent.



- ❖ **Source:** Distilled water, distilled from fractional distillation method in Lab.

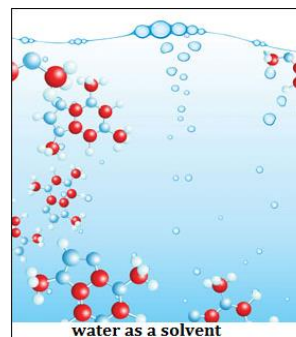
❖ **Purification:** Water was first deionised and then distilled in an all glass distilling set along with alkaline  $KMnO_4$  solution to remove any organic matter therein. The doubly distilled water was finally distilled using an all glass distilling

<b>WATER</b>	
<i>Appearance</i>	:Liquid
<i>Molecular Formula</i>	: $H_2O$
<i>Molecular Weight</i>	:18.02 $g \cdot mol^{-1}$
<i>Density</i>	:0.99713 $g \cdot cm^3$
<i>Viscosity</i>	:0.891 $mP \cdot s$
<i>Refractive Index</i>	:1.3333
<i>Ultrasonic Speed</i>	:1500.0 $m \cdot s^{-1}$
<i>Dielectric Constant</i>	:78.35 at 298.15K

set. Precautions were taken to prevent contamination from CO<sub>2</sub> and other impurities. The triply distilled water had specific conductance less than  $1 \times 10^{-6} \text{ S}\cdot\text{cm}^{-1}$ .

❖ **Application:**

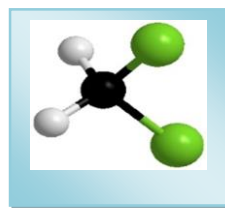
Water is widely used in chemical reactions as a solvent or reactant and less commonly as a solute or catalyst. In inorganic reactions, water is a common solvent, dissolving many ionic compounds. Supercritical water has recently been a topic of research. Oxygen saturated supercritical water combusts organic pollutants efficiently. It is also use in various industries.



It is an excellent solvent, generally called the universal solvent, due to the marked polarity and its tendency of forming hydrogen bonds with other molecules. Water is the main component of life in this earth. Not only a high percentage of living bodies, both plants and animals are found in water, all life on earth is thought to have arisen from water and the bodies of all living organisms are composed mostly of water. About 70 to 90 percent of all organic substance is water. The chemical reactions in all plants and animals that support life take place in water medium. Water not only provides the medium to make these life sustaining reactions possible, but water itself is often an important reactant or product of all these reactions. In short, the chemistry of life is nothing but the “water chemistry.”

➤ **Dichloromethane (DCM):**

Dichloromethane (DCM, or methylene chloride) is an organic compound with the formula CH<sub>2</sub>Cl<sub>2</sub>. This is colorless, volatile liquid with a moderately sweet smelling. This is widely used as a solvent. Although it is not miscible with water, it is miscible with many organic solvents.[10] One of the most well-known applications of dichloromethane is in the drinking bird heat engine.



<b>Dichloromethane</b>	
<i>Appearance</i>	: Colourless Liquid
<i>Molecular Formula</i>	: CH <sub>2</sub> Cl <sub>2</sub>
<i>Molecular Weight</i>	: 84.93 g·mol <sup>-1</sup>
<i>Density</i>	: 1.3266g·cm <sup>3</sup>
<i>Viscosity</i>	: 0.43mP·s
<i>Refractive Index</i>	: 1.4244
<i>Dielectric Constant</i>	: 8.93 at 298.15 K

❖ **Source:** Merck, India.

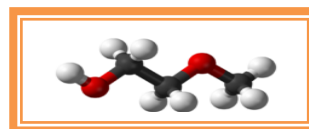
❖ **Purification:** Dichloromethane (DCM) obtained from Merck, India was used after further purification. It was distilled from  $P_2O_5$  and then from  $CaH_2$  in an all-glass distillation apparatus [1].

❖ **Application:**

Dichloromethane is used as a solvent for many different purposes such as DCM's volatility and ability to dissolve a wide range of organic compounds makes it a useful solvent for many chemical processes. It is widely used as a paint stripper and a degreaser. In the food industry, it has been used to decaffeinate coffee and tea as well as to prepare extracts of hops and other flavorings. Its volatility has led to its use as an aerosol spray propellant and as a blowing agent for polyurethane foams.

➤ **Acetonitrile (ACN):**

Acetonitrile is the colourless liquid and of the simplest organic nitrile. It is produced mainly as a byproduct of acrylonitrile manufacture.



❖ **Source:** Merck, India.

❖ **Purification:** Acetonitrile (ACN) obtained from Merck, India was used after further purification. It was distilled from  $P_2O_5$  and then from  $CaH_2$  in an all-glass distillation apparatus [1]. The middle fraction was collected. About 99% purified acetonitrile with specific conductivity  $0.8 - 1.0 \times 10^{-8} \text{ S cm}^{-3}$  was obtained. The purity of the liquid was checked by measuring its density and viscosity which were in good agreement with the literature values [1,2]

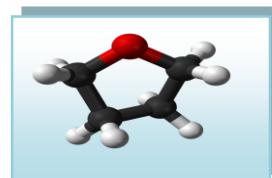
<b>Acetonitrile</b>	
<i>Appearance</i>	: Colourless Liquid
<i>Molecular Formula</i>	: $CH_3CN$
<i>Molecular Weight</i>	: $41.05 \text{ g} \cdot \text{mol}^{-1}$
<i>Density</i>	: $0.786 \text{ g} \cdot \text{cm}^3$
<i>Viscosity</i>	: $0.346 \text{ mP} \cdot \text{s}$
<i>Refractive Index</i>	: 1.3441
<i>Ultrasonic Speed</i>	: $1282.6 \text{ m} \cdot \text{s}^{-1}$
<i>Dielectric Constant</i>	: 35.95 at 298.15 K

❖ **Application:**

It is widely used in electrochemical cells industry as it has relatively high dielectric constant and the ability to dissolve electrolytes more efficiently. For similar reasons it is a popular solvent in cyclic voltammetry. Its low viscosity and low chemical reactivity make it a popular choice for liquid chromatography. Acetonitrile plays a considerable role as a solvent for manufacturing DNA oligonucleotides from its monomers. Industrially, it is used as a solvent in the purification of butadiene and in the manufacture of pharmaceuticals and photographic film. Acetonitrile is a common two-carbon building block in organic synthesis as in the production of pesticides to perfumes.

➤ **Tetrahydrofuran (THF):**

Tetrahydrofuran (THF) is an organic compound with the formula  $(\text{CH}_2)_4\text{O}$ . The compound is classified as heterocyclic compound, specifically a cyclic ether. It is a colorless, water-miscible organic liquid with low viscosity. THF has an odor similar to acetone. It is mainly used as a precursor to polymers. Being polar and having a wide liquid range, THF is a versatile solvent.



❖ **Source:** Merck, Indian.

❖ **Purification:** Tetrahydrofuran (THF), Merck, Indian was kept several days over potassium hydroxide (KOH), refluxed for 24 h and distilled over lithium aluminium hydride ( $\text{LiAlH}_4$ ) described earlier [3]. The purified solvent had a boiling point of 339 K and a specific conductance of  $0.81 \times 10^{-6} \text{ S cm}^{-3}$ . The density and viscosity of the purified solvent were in good agreement with the literature data [4,5] as shown in Table IV.1. The purity of the solvent was  $\geq 98.9\%$ .

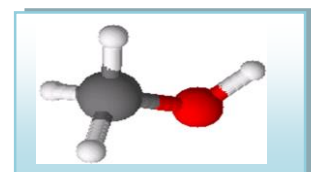
<b>Tetrahydrofuran</b>	
<i>Appearance</i>	: Colourless Liquid
<i>Molecular Formula</i>	: $\text{C}_4\text{H}_8\text{O}$
<i>Molecular Weight</i>	: $72.11 \text{ g}\cdot\text{mol}^{-1}$
<i>Density</i>	: $0.88074 \text{ g}\cdot\text{cm}^3$
<i>Viscosity</i>	: $0.48 \text{ mP}\cdot\text{s}$
<i>Refractive Index</i>	: 1.4072
<i>Ultrasonic Speed</i>	: $1279.0 \text{ m}\cdot\text{s}^{-1}$
<i>Dielectric Constant</i>	: 7.58 at 298.15 K

❖ **Application:**

The main application of THF is as an industrial solvent for PVC and in varnishes. It is an aprotic solvent with a moderately polar solvent and can dissolve a wide range of non-polar and polar chemical compounds. THF is a popular solvent in the laboratory when a moderately higher-boiling ethereal solvent is required and its water miscibility is not an issue. THF is often used in polymer science as dissolve polymers prior to determining their molecular mass using gel permeation chromatography, to PVC as well and thus it is the main ingredient in PVC adhesives. For liquefying old PVC cement this is widely used and often to degrease metal parts it is used industrially. THF is also used as a component in mobile phases for reversed-phase liquid chromatography.

➤ **Methanol (MeOH):**

Methanol, also known as methyl alcohol, wood alcohol, wood naphtha or wood spirits, is the simplest alcohol, and is a light, volatile, colourless, flammable, liquid with a distinctive odour that is very similar to but slightly sweeter than ethanol (drinking alcohol).

❖ **Source:** Merck, India.

❖ **Purification:** It was passed through Linde Å molecular sieves and then distilled [6].

❖ **Application:**

The largest use of methyl alcohol by far is in making other chemicals. Methanol is a traditional denaturant for ethanol, thus giving the term methylated spirit. Methanol is also used as a solvent, and as an antifreeze in pipelines. In some waste water treatment plants, a small amount of methanol is added to waste water to provide a food source of

<b>Methanol</b>	
<i>Appearance</i>	: Colourless Liquid
<i>Molecular Formula</i>	: CH <sub>4</sub> O
<i>Molecular Weight</i>	: 32.04 g·mol <sup>-1</sup>
<i>Density</i>	: 0.7866 g·cm <sup>3</sup>
<i>Viscosity</i>	: 0.5445 mP·s
<i>Refractive Index</i>	: 1.3284
<i>Ultrasonic Speed</i>	: 1103.0 m·s <sup>-1</sup>
<i>Dielectric Constant</i>	: 32.6 at 298.15 K

carbon for the denitrifying bacteria, which converts nitrates to nitrogen to reduce the denitrification of sensitive aquifers. Methanol is used on a limited basis to fuel internal combustion engines. Methanol is also useful as an energy carrier. It is easier to store than hydrogen, burns cleaner than fossil fuels, and is biodegradable.

## III.2. EXPERIMENTAL METHODS

### III.2.1 Preparation of Solutions

A stock solution for each salt was prepared by mass (digital electronic analytical balance, Mettler Toledo, AG 285, Switzerland), and the working solutions were obtained by mass dilution of the stock solution. The uncertainty of concentration (molarity or molality) of different working solutions was evaluated to be  $\pm 0.0002$ .

### III.2.2 Preparation of Multicomponent Liquid Mixtures

The binary and multicomponent liquid mixtures can be prepared by any one of the methods discussed below:

(a) **Mole fraction**

(b) **Weight fraction**

(c) **Volume fraction**

**(a) Mole fraction:** The mole fraction ( $x_i$ ) of the multicomponent liquid mixtures can be prepared using the following relation:

$$x_i = \frac{(w_i / M_i)}{\sum_{i=1}^n (w_i / M_i)}$$

Where  $w_i$ , and  $M_i$  are weight and molecular weight of  $i^{\text{th}}$  component, respectively.

The values of  $i$  depends on the number of components involved in the formation of a mixture.

**(b) Weight fraction:** The mole fraction ( $w_i$ ) of the multicomponent liquid mixtures can be prepared using the following relation:

$$w_i = \frac{(x_i / M_i)}{\sum_{i=1}^n (x_i M_i)}$$

**(c) Volume fraction:** The volume fraction ( $\phi_i$ ) of the multicomponent liquid mixtures can be prepared by following employing three methods:

**i. Using volume:** The volume fraction ( $\phi_i$ ) of the multicomponent liquid mixtures can be prepared by following relation

$$\phi_i = \frac{V_i}{\sum_{i=1}^n V_i}$$

Where  $V_i$ , is the volume of pure liquid  $i$ .

**ii. Using molar volume:** The volume fraction ( $\phi_i^l$ ) of the multicomponent liquid mixtures can be prepared by following relation

$$\phi_i^l = \frac{x_i V_{mi}}{\sum_{i=1}^n (x_i V_{mi})}$$

Where  $V_{mi}$  is the molar volume of pure liquid  $i$ .

**iii. Using excess volume:** The volume fraction ( $\phi_i^{ex}$ ) of the multicomponent liquid mixtures can be prepared by following relation

$$\phi_i^{ex} = \frac{x_i V_i}{\sum_{i=1}^n (x_i V_i) + V^E}$$

Where  $V^E$  is the excess volume of the liquid mixture.

### III.2.3 Measurements of Experimental Properties

#### III.2.3.1 Mass Measurement

Using digital electronic analytical balance Mettler Toledo, AG 285, Switzerland mass in different cases were measured.

It can measure mass to a very high precision and accuracy. The weighing pan of a high precision (0.0001g) is inside a transparent enclosure with doors so that dust does not collect and so any air currents in the room do not affect the balance's operation.



#### Instrument Specification:

Readability	: 0.1 mg/ 0.01mg
Maximum capacity	: 210 g/81g/41g
Taring range	: 0... 210 g
Repeatability	: 0.1 mg/ 0.05 mg
Linearity	: $\pm 0.2$ mg/ $\pm 0.1$ mg
Stabilization time	: 3 s/ 15 s
Adjustment with external weights	: 200 g
Sensitivity	: $\pm 0.003\%$
Display	: LCD
Interface	: Local CAN universal interface
Weighing	: $\Phi$ 85 mm, stainless steel
Effective height above pan	: 240 mm
Dimensions(w/d/h)	: 205×330×310 mm
Net wt/with packaging	: 4.9 kg/7.25 kg

#### III.2.3.2 Conductivity Measurement

Conductivity measurement was done using Systronics Conductivity TDS meter-308. It is a microprocessor based instrument used for measuring specific conductivity of solutions. It can provide both automatic and manual temperature compensation.





***Systronic-308 Conductivity Bridge***

The conductance measurements were carried out on this conductivity bridge of accuracy  $\pm 0.01\%$ , using a dip-type immersion conductivity cell, CD-10 having a cell constant of approximately  $(0.1 \pm 0.001) \text{ cm}^{-1}$ . Measurements were made in a thermostate water bath maintained at  $T = (298.15 \pm 0.01) \text{ K}$ . The cell was calibrated by the method proposed by Lind et al. [7] and cell constant was measured based on 0.01 M aqueous KCl solution [8]. During the conductance measurements, cell constant was maintained within the range  $1.10\text{--}1.12 \text{ cm}^{-1}$ . The conductance data were reported at a frequency of 1 kHz with the accuracy of  $\pm 0.3\%$ . The conductivity cell was sealed to the side of a  $500 \text{ cm}^3$  conical flask closed by a ground glass fitted with a side arm through which dry and pure nitrogen gas was passed to stop admittance of air into the cell during the addition of solvent or solution. The measurements were made in a thermostatic water bath maintained at the required temperature with an accuracy of  $\pm 0.01 \text{ K}$  by means of mercury in glass thermos-regulator[9].

**Instrument Specifications:**

Frequency	: 100 Hz or 1 KHz Automatic
Conductivity	
Range	: 0.1 $\mu$ S to 100 mS. (6 decadic range)
Accuracy	: $\pm 1\%$ of F.S. $\pm 1$ digit
Resolution	: 0.001 $\mu$ S
TDS	
Range	: 0.1 ppm to 100 ppt. (6 decadic range)
Accuracy	: $\pm 1\%$ of F.S. $\pm 1$ digit
Temperature	
Range	: 0°C to 100°C (Auto/Manual)
Accuracy	: $\pm 0.2$ °C $\pm 1$ digit
Resolution	: 0.1 °C
Cell Constant	: Acceptable from 0.1 to 5.0
Auto Temp. Compensation	: 0°C to 100°C with PT 100 sensor
Manual Temp. Compensation	: 0°C to 60°C user selectable
Conductivity temp. Co-efficient	: 0.0% to 9.9% user selectable
Display	: 7 digits, 7 segment LEDs (3 digits for TEMP/TEMPCO 4 digits for Conductivity/TDS) With automatic decimal point selection
TDS-factor	: 0.00 to 9.99 user selectable
Printer Port	: Epson compatible 80 Column Dot Matrix
Power	: 230V AC, $\pm 10\%$ , 50 Hz
Dimensions	: 250(W) $\times$ 205(D) $\times$ 75(H)
Weight	: 1.25 Kg (Approx.)
Accessories	: i) Conductivity cell, cell constant 0.1 ii) Conductivity cell, cell constant 1.0 iii) Temp. Probe (PT-100 sensor) iv) Stand & Clamp

Solutions were prepared by weight precise to  $\pm 0.02\%$ . The weights were taken on a Mettler electronic analytical balance (AG 285, Switzerland). The molarity being converted to molality as required. Several independent solutions were prepared and runs were performed to ensure the reproducibility of the results. Due correction was made for the specific conductance of the solvents at desired temperatures.

### III.2.3.3 Density Measurement

The density measurement was performed with the help of Anton Paar DMA 4500M digital density-meter with a precision of  $\pm 0.0005 \text{ g}\cdot\text{cm}^{-3}$ .



**Anton Paar DMA 4500M digital density-meter**

In the digital density meter, the mechanic oscillation of the U-tube is e.g. electromagnetically transformed into an alternating voltage of the same frequency. The period  $\tau$  can be measured with high resolution and stands in simple relation to the density  $\rho$  of the sample in the oscillator:

$$\rho = A \cdot \tau^2 - B \quad (\text{III.1})$$

A and B are the respective instrument constants of each oscillator. The values of A and B are determined by the calibration with the solutions of two different substances of known densities  $\rho_1$  and  $\rho_2$ . Modern instruments calculate and store the constants A and B after the two calibration measurements, which are mostly performed with air and water. They produce suitable values to balance various influences during the measurement, e.g., the influence of the sample's viscosity and the non-linearity caused by the measuring instrument's finite mass. The instrument was calibrated by triply-distilled water and dry air.

**Instrument Specification:**

Density	: 0 to 1.5 g.cm <sup>-3</sup>
Temperature	: 15°C to 25°C
Pressure	: 0 to 6 bar
<b>Repeatability Standard Deviation</b>	
Density	: 0.00001 g.cm <sup>-3</sup>
Temperature	: 0.01 °C
Additional information	
Minimum sample volume	: approx. 2 ml
Dimensions (L×W×H)	: 400×225×231 mm
Weight	: approx. 15 kg
Automatic bubble detection	: yes
Interfaces	: 2×CAN
Power	: Supplied by the master instrument

**III.2.3.4 Viscosity Measurement**

**By Brookfield DV-III Ultra Programmable Rheometer:** The viscosities ( $\eta$ ) were measured using a Brookfield DV-III Ultra Programmable Rheometer with fitted spindle size-42. The viscosities were obtained using the following equation

$$\eta = (100 / RPM) \times TK \times \text{torque} \times SMC$$

Where, *RPM*, *TK* (0.09373) and *SMC* (0.327) are the speed, viscometer torque constant and spindle multiplier constant, respectively. The calibration of the instrument was done using the standard viscosity sample solutions supplied with the instrument, water and aqueous CaCl<sub>2</sub> solutions [10]. The temperature was maintained to within  $\pm 0.01^\circ\text{C}$  using Brookfield Digital TC-500 thermostat bath. This instrument provides viscosity values with an accuracy of  $\pm 1\%$ . Each measurement was reported as an average of three separate reading with a precision of 0.3 %.



**Instrument Specifications:**

<i>Speed Range</i>	<i>: 0-250 RPM, 0.1 RPM increments</i>
<i>Viscosity Accuracy</i>	<i>: <math>\pm 1.0\%</math> of full scale range for a specific spindle running at a specific speed.</i>
<i>Temperature sensing range</i>	<i>: <math>-100^{\circ}\text{C}</math> to <math>300^{\circ}\text{C}</math> (<math>-148^{\circ}\text{F}</math> to <math>572^{\circ}\text{F}</math>)</i>
<i>Temperature accuracy</i>	<i>: <math>\pm 1.0^{\circ}\text{C}</math> from <math>-100^{\circ}\text{C}</math> to <math>150^{\circ}\text{C}</math> <math>\pm 2.0^{\circ}\text{C}</math> from <math>+150^{\circ}\text{C}</math> to <math>300^{\circ}\text{C}</math></i>
<i>Analog Torque Output</i>	<i>: 0 - 1 Volt DC (0 - 100% torque)</i>
<i>Analog Temperature Output</i>	<i>: 0 - 4 Volts DC (10mv / <math>^{\circ}\text{C}</math>)</i>

### III.2.3.5 Refractive Index Measurement

Refractive index was be measure with the help of Digital Refractometer (Mettler Toledo 30GS).

The instrument was calibrated using double-distilled water, toluene, cyclohexane, and carbon tetrachloride at defined temperature. The accuracy of the instrument is  $\pm 0.0005$ . A few drops of the sample solution were placed onto the measurement cell and the value of refractive index was taken. As refractive index is dependent on temperature, refractometer is designed to determine the temperature to produce the exact value.



#### Specifications-Refracto 30GS- extended RI measuring range

<i>Model</i>	: <i>Refracto 30GS</i>
<i>Measurement range</i>	: <i>1.32 -1.65</i>
<i>Resolution</i>	: <i>0.0001</i>
<i>Accuracy</i>	: <i>+/- 0.0005</i>
<i>Measurement range BRIX</i>	: <i>0 - 85 Brix%</i>
<i>Resolution</i>	: <i>0.1 Brix%</i>
<i>Accuracy</i>	: <i>+/- 0.2 Brix%</i>
<i>Temperature range</i>	: <i>10 - 40°</i>
<i>Resolution of temperature</i>	: <i>0.1°</i>
<i>display</i>	: <i>°C or °F</i>
<i>Trade Name</i>	: <i>51324660</i>

The ratio of the speed of light in a vacuum to the speed of light in another substance is defined as the index of refraction (aka refractive index or  $n_D$ ) for the substance.

$$\text{Refractive index of the substance } (n_D) = \frac{\text{Speed of light in vacuum}}{\text{Speed of light in substance}} \quad (\text{III.5})$$

$$\frac{V_A}{V_B} = \frac{\sin \theta_A}{\sin \theta_B} = \frac{n_B}{n_A} \quad (\text{III.6})$$

Hence, without measuring the speed of light in a sample its index of refraction can easily be determined. Measuring the angle of refraction and refraction index of layer in contact with the sample it determines the refractive index of the sample accurately [11]. Nearly all refractometers utilize this principle, but may differ in their optical design.

Whenever light changes speed as it crosses a boundary from one medium into another its direction of travel also changes, i.e., it is refracted (Figure 1). (In the special case of the light traveling perpendicular to the boundary there is no change in direction upon entering the new medium.) The relationship between light's speed in the two mediums ( $v_A$  and  $v_B$ ), the angles of incidence ( $\theta_A$ ) and refraction ( $\theta_B$ ) and the refractive indexes of the two mediums ( $n_A$  and  $n_B$ ) is shown below:

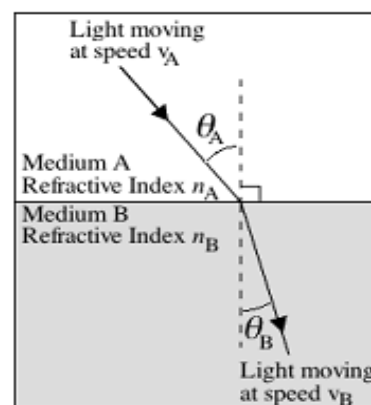


**Figure 1.** Light crossing from any transparent medium into another in which it has a different speed, is refracted, i.e., bent from its original path (except when the direction of travel is perpendicular to the boundary). In the case shown, the speed of light in medium A is greater than the speed of light in medium B

A light from its source is projected towards the illuminating prism with ground bottom surface that means roughened like a ground-glass joint so that each point on this surface can be regarded as producing light rays to be travelled in all directions. As in figure2 light propagating from point A to point B with largest angle of incidence ( $q_i$ ) and consequently the largest possible angle of refraction ( $q_r$ ) for a particular sample. Rest of the rays of light which go into the refracting prism with  $q_r$  and consequently get revealed to the left of point C. Thus, the detector positioned on the back side of the refracting prism would show a light region to the left and a dark region to the right.

### III.2.3.6 Surface Tension Measurement

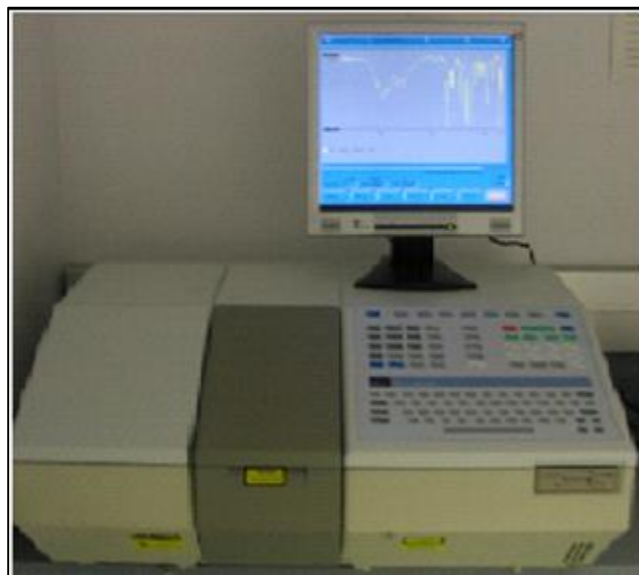
Surface tension were measured by using Digital Tensiometer KRUSS K9 (Germany). The tensiometer is a precision instrument which will only perform reliably on a solid and vibration-free base. It places the same demands on its surroundings as a laboratory balance with a resolution of 0.1 mg. In addition surface tension measurements require a clean and dust-free atmosphere as atmospheric pollutants could directly falsify the results.



### III.2.4.7 FTIR Measurement

Infrared spectra were recorded in 8300 FTIR spectrometer (Shimadzu, Japan). It measures the intensity of light passing through the blank ( $I_0$ ) and measures the intensity of light ( $I$ ) passing through the sample.

The blank solution is identical to the sample solution only differing in the case that it does not contain the substrate which absorbs light. (In practice, instrument





measures the power rather than the intensity of the light. The power is the energy per second, which is the product of the intensity (photons per second) and the energy per photon. The experimental data is used to analyse two quantities: the transmittance ( $T$ ) and the absorbance ( $A$ ).

$$T = \frac{I}{I_0}; \quad A = -\log_{10} T \quad (\text{III.7})$$

The fraction of light in the original beam passing through the sample and reaches the detector is the transmittance.

#### **III.2.4.8 UV-VIS Spectra Measurement**

Compounds that absorb Ultraviolet and/or visible light have characteristic absorbance curves as a function of wavelength. Absorbance of different wavelengths of light occurs as the molecules move to higher energy states.



The UV-VIS spectrophotometer uses two light sources, a deuterium (D<sub>2</sub>) lamp for ultraviolet light and a tungsten (W) lamp for visible light. After bouncing off a mirror, the light beam passes through a slit and hits a diffraction grating. The grating can be rotated allowing for a specific wavelength to be selected. At any specific orientation of the grating, only monochromatic (single wavelength) successfully passes through a slit. A filter is used to remove unwanted higher orders of diffraction. There is a half mirror where half of the light is reflected and the other half passes through. Before the half mirror the light beam hits a second mirror to avoid the splitting. One of the beam is allowed to pass through a reference cuvette (which contains the solvent only), the other passes through the sample cuvette. The intensities of the light beams are then measured at the end. Regarding this the Beer-Lambert law has been stated below.

### Beer-Lambert Law

The change in intensity of light ( $dI$ ) after passing through a sample should be proportional to the following:

- (i) Path length ( $b$ ), the longer the path, more photons should be absorbed
- (ii) Concentration ( $c$ ) of sample, more molecules absorbing means more photons absorbed
- (iii) Intensity of the incident light ( $I$ ), more photons means more opportunity for a molecule to see a photon. Thus,  $dI$  is proportional to  $bcl$  or  $dI/I = -kbc$  (where  $k$  is a proportionality constant, the negative sign is shown because this is a decrease in intensity of the light, this makes  $b$ ,  $c$  and  $I$  always positive. Integration of the above equation leads to Beer-Lambert's law [12]:

$$- \ln I/I_0 = kbc \quad (\text{III.8})$$

$$- \log I/I_0 = 2.303kbc \quad (\text{III.9})$$

$$\epsilon = 2.303k \quad (\text{III.10})$$

$$A = - \log I/I_0 \quad (\text{III.11})$$

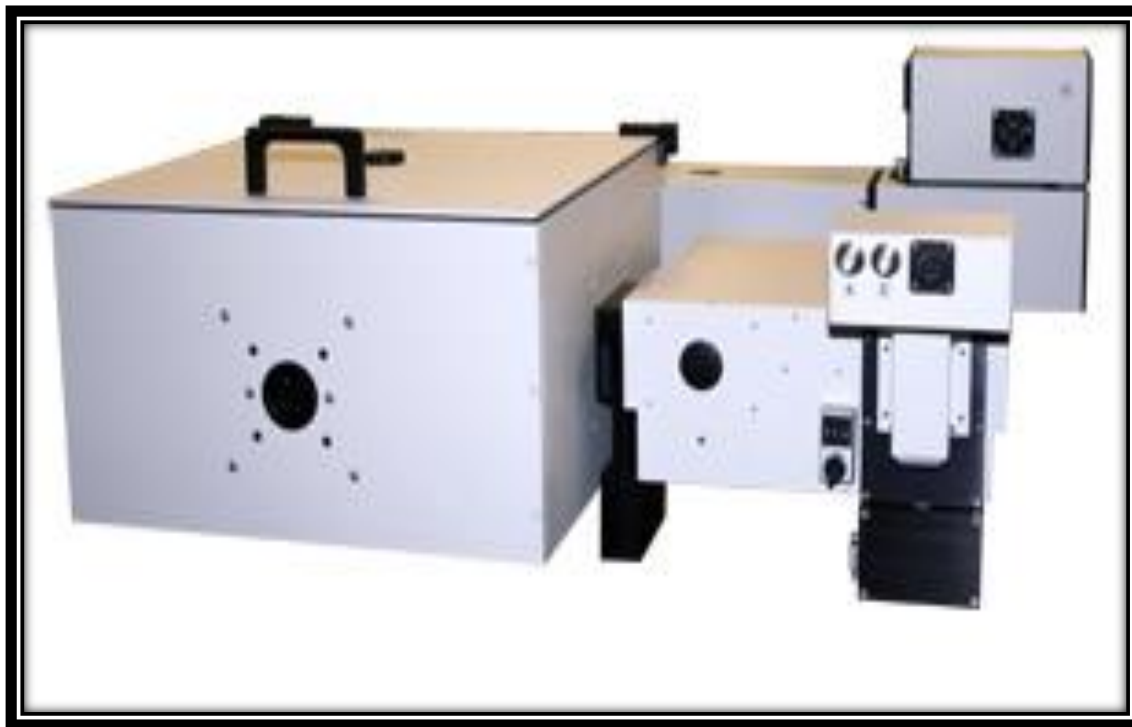
$$A = \epsilon bc \quad (\text{III.12})$$

$A$  is defined as absorbance and it is found to be directly proportional to the path length,  $b$  and the concentration of the sample,  $c$ . The extinction coefficient is characteristic of the substance under study and of course is a function of the wavelength.

**III.2.3.9 Quanta Master 40 spectrofluorometer**

Fluorescence is the emission of light from a molecule resulting from a transition from one electronic state to a lower electronic state of the same multiplicity.

Detection Limit	460 attomolar fluorescein in 0.1 M NaOH
Signal to Noise Ratio	10,000:1 or better (350 nm excitation, 5 nm spectral bandpass, 1 s integration time)
Data Acquisition Rate	50,000 points/sec. to 1 point/100 sec
Inputs	4 analog (+/- 10 volts)
	2 photon counting (TTL)
	1 analog reference channel (+/- 10 volts)
	2 TTL
Outputs	2 analog (+/- 10 volts)
	2 TTL
Emission Range	185 nm to 680 nm (optional to 900 nm)
Light Source	High efficiency continuous Xenon arc lamp
Monochromators	Czerny-Turner design
Focal Length	200 mm
Excitation Grating	1200 line/mm 300 nm blaze
Emission Grating	1200 line/mm 400 nm blaze
Optional Grating	75 to 2400 line/mm and holographic models available
Bandpass	0 to 24 nm, continuously adjustable (computer control available)
Wavelength Accuracy	+/- 0.5 nm
Wavelength Resolution	0.06 nm
Detection	Photon counting/analog
System Control	Computer interface with spectroscopy software
Dimensions	38 x 30 inches



The most commonly observed fluorescence from organic molecules is caused by a transition from an excited singlet state to the ground singlet state.

Molecules have various states referred to as energy levels. Fluorescence spectroscopy is associated with electronic and vibrational states in principal. Generally, the molecules of a particular species consist of ground electronic state and an excited electronic state and a number of vibrational states within these two electronic states.

The fluorescence spectroscopy consist a number of steps. First of all the species is excited from its ground electronic state to one of the different vibrational states of higher energy. The excited molecules may collide with other molecules and lose vibrational energy until it reaches the lowest vibrational state of the ground electronic state. This process is described with a Jablonski diagram. The molecule then emits a photon to fall down to one of the various vibrational levels of the ground electronic state again. As a number of vibrational levels in the ground state are available, the emitted photons will

have frequencies. Thus the analysing of different frequencies, along with their relative intensities, the structure of the various vibrational levels can be determined.

In a typical experiment, the different wavelengths of fluorescent light emitted by a sample are measured using a monochromator, holding the excitation light at a constant wavelength. This is called an *emission spectrum*. An emission map is measured by recording the emission spectra resulting from a range of excitation wavelengths and combining them all together. This is a three dimensional surface data set: emission intensity as a function of excitation and emission wavelengths, and is typically depicted as a contour map.

The QuantaMaster 40 spectrofluorometer has widespread applications. Below are some examples:

- Protein folding/unfolding
- Anisotropy
- FRET
- Chemiluminescence
- Bioluminescence
- Semiconductor Research
- Electroluminescence Measurements
- Photovoltaic Measurements

#### ***III.2.4.10 NMR Spectra Measurement***

As on the strength of the magnetic field the resolution is mainly dependent, the NMR spectrometers are designed with very strong, big and liquid helium-cooled superconducting magnet. Less expensive machines where permanent magnets are used are also available, which still give sufficient performance for certain application such as reaction monitoring and quick checking of samples but resolution is quite low.



The protons of the solvents, as most regular solvents are hydrocarbons, are NMR active. Thus, deuterium (hydrogen-2) is substituted (99+ %). Generally deuteriochloroform ( $\text{CDCl}_3$ ) is used as a solvent. Apart from deuteriochloroform deuterium oxide ( $\text{D}_2\text{O}$ ) and deuterated DMSO ( $\text{DMSO-d}_6$ ) are also used where applicable. While recording the NMR spectra often known solvent residual proton peak was taken as the internal standard where applicable instead of adding tetramethylsilane.

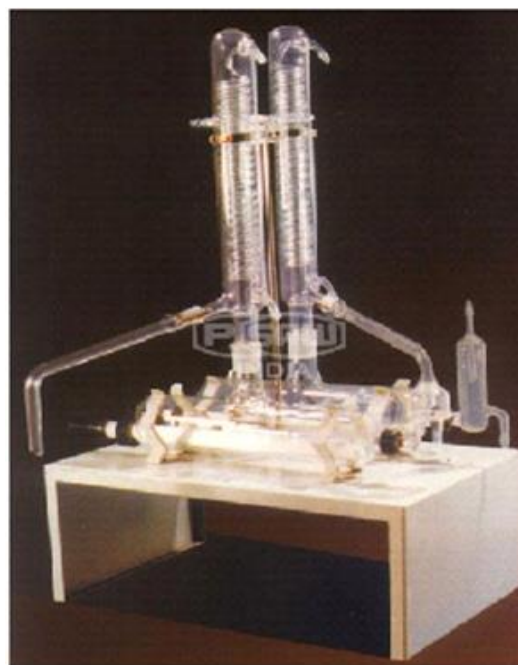
NMR spectra were recorded in  $\text{D}_2\text{O}$  unless otherwise stated.  $^1\text{H}$  NMR spectra were recorded at 300 MHz and 400 MHz using Bruker ADVANCE 300 MHz and Bruker ADVANCE 400 MHz instruments respectively at 298.15K. Signals are quoted as  $\delta$  values in ppm using residual protonated solvent signals as internal standard ( $\text{D}_2\text{O}$ :  $\delta$  4.79 ppm). Data are reported as chemical shift.

### ➤ **Other Instruments Used:**

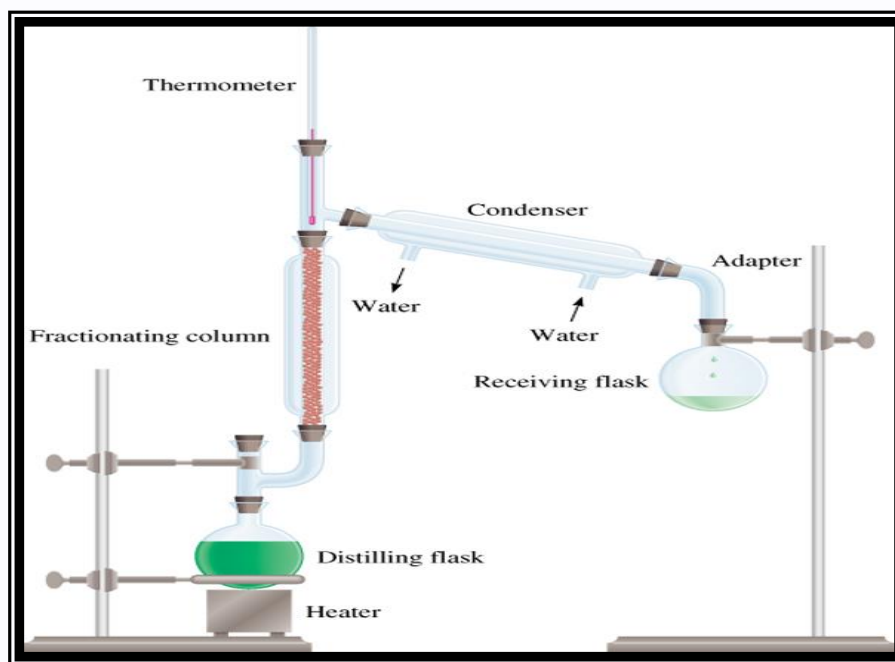
#### **III.2.4.11 Water Distiller**

Water from the natural sources is manually or automatically fed into steaming chamber of the distiller unit's. The steam arises from the steaming chamber is passed through a built-in vent to condenser where the steam gets converted into water which

then passes through and store into a container. Minerals and salts due to high boiling point remains in the boiling chamber as hard deposits or scale. The distilled water is then collected in a storage tank. If the unit is an automatic model, it is set to operate to fill the storage tank. The distillation apparatus contains a flask with heating elements embedded in glass and fused in spiral type coil internally of the bottom and tapered round glass, joints at the top double walled condenser with B-40/B-50 ground glass joints, suitable to work on 220 volts, 50 cycles AC supply.



Water distillation units produce highly treated and disinfected water for laboratory usage. The distillation process removes minerals and microbiological contaminants and can reduce levels of chemical contaminants.



**Fractional Distillation Apparatus**

### **III.2.4.12 Thermostat Water Bath (Science India, Kolkata):**

Temperature was controlled using thermostatic water bath and in which the experiments were also carried out. The temperature was maintained with an accuracy of  $\pm 0.01$  K of the desired temperature.



***Thermostat water bath***

Laboratory water bath is a system in which a vessel containing the material to be heated is placed into or over the one containing water and to quickly heat it. These laboratory equipment supplies are available in different volumes and construction with both digital and analogue controls and greater temperature uniformity, durability, heat retention and recovery. The chambers of water bath lab products are manufactured using rugged, leak proof and highly resistant stainless steel and other lab supplies.



# CHAPTER-IV

## **NMR, SURFACE TENSION AND CONDUCTANCE STUDY TO INVESTIGATE HOST-GUEST INCLUSION COMPLEXES OF THREE SEQUENTIAL IONIC LIQUIDS WITH $\beta$ -CYCLODEXTRIN IN AQUEOUS MEDIA**

### **IV.1. INTRODUCTION**

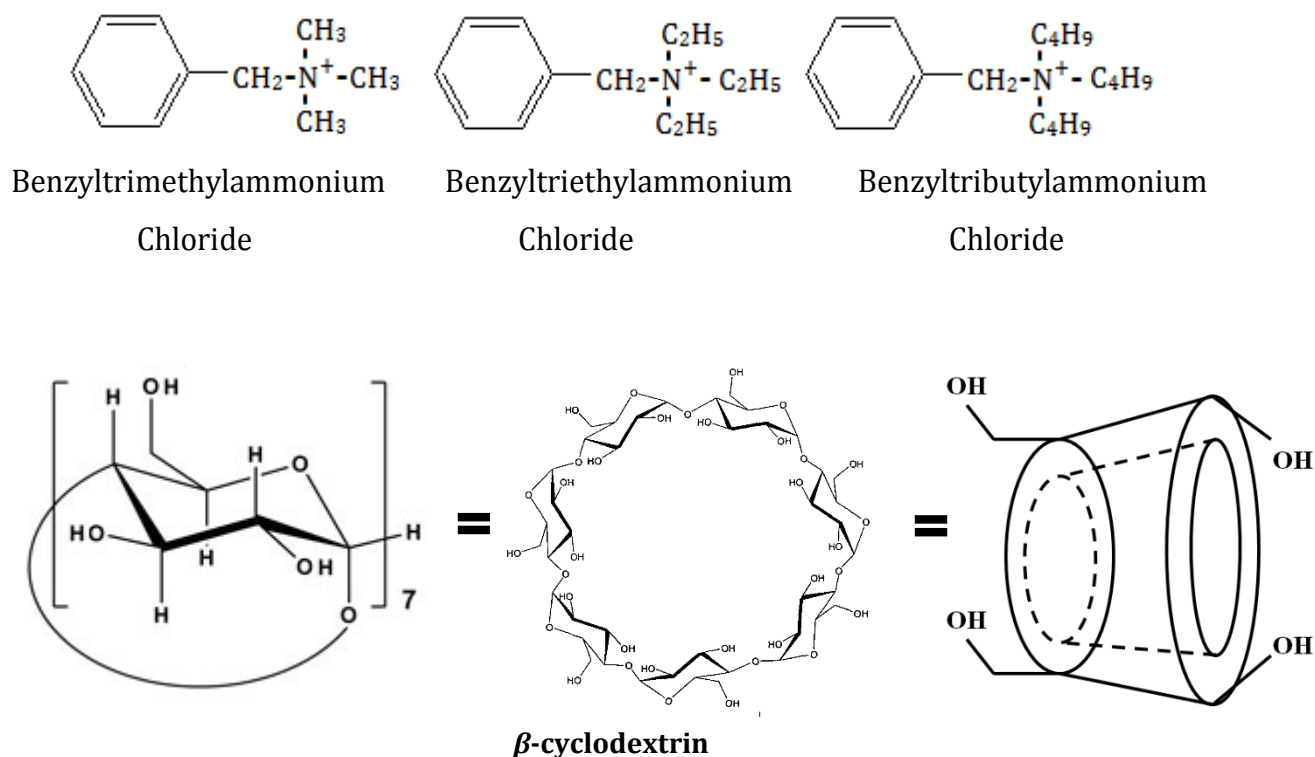
Supramolecular assembly is the association of guest molecules into the inner cavity of a host molecule by noncovalent bonds under equilibrium conditions [1]. Cyclodextrin seems to be the most promising host molecule to form inclusion complexes [2].  $\beta$ -Cyclodextrin ( $\beta$ -CD) is a cyclic oligosaccharide (consists of seven  $\alpha$ -D-glucopyranose units, linked by glycosidic bonds  $\alpha$ -1,4 obtained as the main product from the enzymatic conversion of the starch [3-6]. Due to lack of free rotation about the glycosidic bond,  $\beta$ -CD (as the  $\alpha$ - and  $\gamma$ -CDs) has a unique spatial configuration, showing a cylindrical hollow truncated cone shape; cavity with 6.0Å of width and 7.9Å of height, has a hydrophobic character, while the rims are hydrophilic: the wider one, with fourteen primary hydroxyl groups (-OH), and a narrower one with, the seven secondary OH groups (-CH<sub>2</sub>OH) (Scheme IV.1). These structural features give all the fitting and encapsulating properties to  $\beta$ -CD, for forming inclusion complexes with molecules that fit into the hydrophobic cavity.

Cationic ionic liquids are the prominent surface active agents with positively charged hydrophilic head group and a hydrophobic tail group, have attracted immense interest in the development of methods for separation, purification, extraction of DNA; and also been tested for gene delivery and gene transfection that involve in current clinical trials based on gene therapy [7, 8].

The driving force of inclusion complex formation is the displacement of water molecules by more hydrophobic guest molecules present in the solution to attain an apolar-apolar association [2]. The surface active ionic liquids are form inclusion complex

with  $\beta$ -CD; may be applied in industries, agriculture, textile, detergent, food, cosmetics and the drug or pharmaceutical [9, 10], as antibacterial, antistatic, corrosion inhibitory, dispersants, emulsifying, wetting and solubilizing agent's etc [9, 11, 12]. In addition to these industrial applications, CDs are related to many interesting topics, such as molecular recognition and self-assembly, molecular encapsulation, chemical stabilization, and intermolecular interactions [13, 14].

However, to the best of our knowledge, no work has yet been done in as our chosen system. In this paper, size, shape, structural effect of ionic liquids in the formation of the inclusion complexes have been studied quantitatively and qualitatively to find the nature of ionic host-guest inclusion complexes of sequential cationic room temperature surface active ionic liquids, benzyltrialkylammonium chloride  $[(C_6H_5CH_2)N(C_nH_{2n+1})_3]Cl$ ; where  $n=1,2,4$ ] (**Scheme IV.1**) with  $\beta$ -cyclodextrin in aqueous media using surface tension, conductance and NMR study.



**Scheme IV.1:** Molecular structure of cationic surfactant and  $\beta$ -cyclodextrin.

## IV.2. EXPERIMENTAL SECTION

### IV.2.1 Reagents

The cationic surfactants benzyltrimethylammonium chloride (97%), benzyltriethylammonium chloride (99%), benzyltributylammonium chloride (98%) and  $\beta$ -cyclodextrin (97%) were bought from Sigma-Aldrich, Germany and used as purchased.

### IV.2.2 Instrumentations

Prior to the start of the experimental work solubility of the chosen cyclodextrins in triply distilled and degassed water (with a specific conductance of  $1 \times 10^{-6} \text{ S} \cdot \text{cm}^{-1}$ ) and title compounds *viz.*, cationic surfactant in aqueous  $\beta$ -cyclodextrin have been precisely checked and it was observed that the selected cationic surfactant freely soluble in all proportion of aq.  $\beta$ -cyclodextrins. All the stock solutions of the cationic surfactant were prepared by mass (weighed by Mettler Toledo AG-285 with uncertainty  $0.0003\text{g}$ ), and then the working solutions were obtained by mass dilution at  $298.15 \text{ K}$ .

The surface tension experiments were done by platinum ring detachment method using a Tensiometer (K9, KRÚSS; Germany) at  $298.15 \text{ K}$ . The accuracy of the measurement was within  $\pm 0.1 \text{ mN} \cdot \text{m}^{-1}$ . Temperature of the system has been maintained by circulating auto-thermostated water through a double-wall glass vessel containing the solution.

The conductance measurements were carried out in a Systronics-308 conductivity bridge of accuracy  $\pm 0.01\%$ , using a dip-type immersion conductivity cell, CD-10 having a cell constant of approximately  $(0.1 \pm 0.001) \text{ cm}^{-1}$  [15]. The measurements were made in an auto-thermostated water bath maintaining the temperature at  $298.15 \text{ K}$  and using the HPLC grade water with specific conductance of  $6.0 \mu\text{S m}^{-1}$ . The cell was calibrated using a  $0.01\text{M}$  aqueous KCl solution. The uncertainty in temperature was  $0.01\text{K}$ .

NMR spectra were recorded in  $\text{D}_2\text{O}$  unless otherwise stated.  $^1\text{H}$  NMR spectra were recorded at  $400 \text{ MHz}$  using Bruker ADVANCE  $400 \text{ MHz}$  instrument at  $298.15\text{K}$ . Signals are quoted as  $\delta$  values in ppm using residual protonated solvent signals as internal standard ( $\text{D}_2\text{O}$ :  $\delta$   $4.79 \text{ ppm}$ ). Data are reported as chemical shift.

### IV.3. RESULTS AND DISCUSSION

#### IV.3.1. Critical Micellization Concentration (CMC)

The micelle forming concentration of the three cationic room temperature ionic liquids was measured by surface tension, ( $\gamma$ ) and molar conductivity ( $\Lambda$ ) in aqueous media.

In **Figure IV.1** the surface tension ( $\gamma$ ) values obtained for the cationic based ionic liquid solution is plotted as a function of the ionic liquid concentration at 298 K. Surface tension decreases with the increase of ionic liquid concentration, reach a minima (called critical micellization concentration, CMC) and the slight increase or taken as almost constant variation with further addition of ionic liquids, have disclosed no effective variation in the surface tension as expected very seriously [16]. The break point in Figure IV.1 demonstrates that the micelle starts to form at the critical micellization concentration (CMC) of  $3.0 \cdot 10^{-3}$ ,  $2.6 \cdot 10^{-3}$ , and  $2.0 \cdot 10^{-3}$  M (**Table IV.1**) for  $[(C_6H_5CH_2)N(CH_3)_3]Cl$ ,  $[(C_6H_5CH_2)N(C_2H_5)_3]Cl$  and  $[(C_6H_5CH_2)N(C_4H_9)_3]Cl$  respectively.

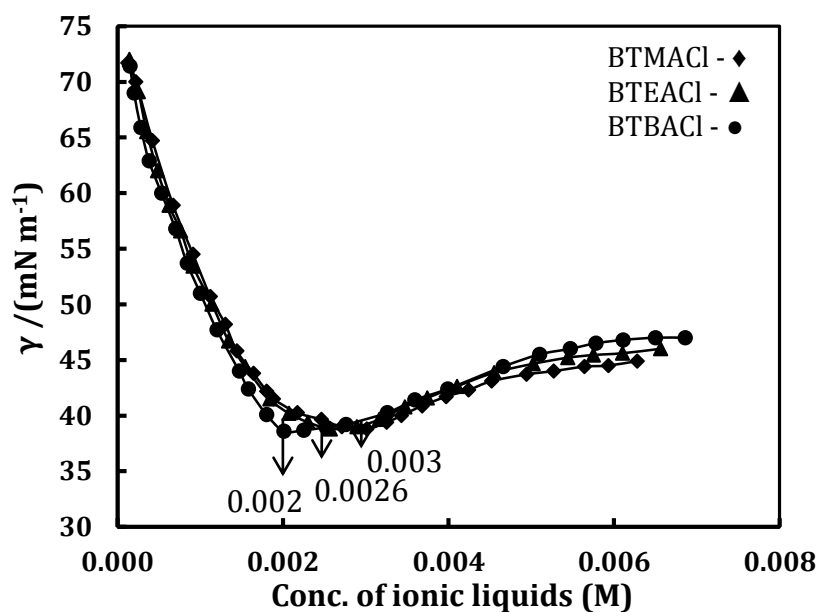


**Figure IV.1:** Plot of surface tension ( $\gamma$ ) with corresponding conc. (M) of ionic liquids.

**Table IV.1:** Molar Conductance ( $\Lambda$ ) and Surface tension ( $\gamma$ ) values with corresponding concentration at the CMC and saturation point of inclusion; and concentration ratio (ratio of inclusion IL:  $\beta$ -CD) at the break point of the surfactants solution (0.01 M) in aqueous  $\beta$ -CD.

Ionic liquids	CMC (M)	$\Lambda_{\text{CMC}}$ (S cm <sup>2</sup> mol <sup>-1</sup> )	Conc. (M)	$\Lambda$ (S cm <sup>2</sup> mol <sup>-1</sup> ) at break point	Conc. ratio (IL: $\beta$ -CD)
[(C <sub>6</sub> H <sub>5</sub> CH <sub>2</sub> )N(CH <sub>3</sub> ) <sub>3</sub> Cl	0.0031	40.31	0.0101	11.90	1 : 1.01
[(C <sub>6</sub> H <sub>5</sub> CH <sub>2</sub> )N(C <sub>2</sub> H <sub>5</sub> ) <sub>3</sub> Cl	0.0029	32.50	0.0103	11.71	1 : 1.03
[(C <sub>6</sub> H <sub>5</sub> CH <sub>2</sub> )N(C <sub>4</sub> H <sub>9</sub> ) <sub>3</sub> Cl	0.0019	18.72	0.0105	12.30	1 : 1.05
Ionic liquids	CMC (M)	$\gamma_{\text{CMC}}$ (mN m <sup>-1</sup> )	Conc. (M)	$\gamma$ (mN m <sup>-1</sup> ) at break point	Conc. ratio (IL: $\beta$ -CD)
[(C <sub>6</sub> H <sub>5</sub> CH <sub>2</sub> )N(CH <sub>3</sub> ) <sub>3</sub> Cl	0.0030	39.1	0.0101	68.0	1 : 1.01
[(C <sub>6</sub> H <sub>5</sub> CH <sub>2</sub> )N(C <sub>2</sub> H <sub>5</sub> ) <sub>3</sub> Cl	0.0026	38.9	0.0102	65.5	1 : 1.02
[(C <sub>6</sub> H <sub>5</sub> CH <sub>2</sub> )N(C <sub>4</sub> H <sub>9</sub> ) <sub>3</sub> Cl	0.0020	38.6	0.0105	63.8	1 : 1.05

The conductance values ( $\Lambda$ ) obtained for the cationic ionic liquid solution is also plotted as a function of the ionic liquid concentration. Conductivity increases monotonically with the increase of the ionic liquid concentration, but after a certain point (called break point) the conductance data have not vary effectively even further addition of ionic liquid. The break point (**Figure IV.2**) at the concentration of  $3.1 \times 10^{-3}$ ,  $2.9 \times 10^{-3}$ , and  $1.9 \times 10^{-3}$  M for [(C<sub>6</sub>H<sub>5</sub>CH<sub>2</sub>)N(CH<sub>3</sub>)<sub>3</sub>Cl], [(C<sub>6</sub>H<sub>5</sub>CH<sub>2</sub>)N(C<sub>2</sub>H<sub>5</sub>)<sub>3</sub>Cl] and [(C<sub>6</sub>H<sub>5</sub>CH<sub>2</sub>)N(C<sub>4</sub>H<sub>9</sub>)<sub>3</sub>Cl] respectively (**Table IV.1**), demonstrates the critical micellization concentration (CMC), where, the micelles starts to form. The point is confirmed by conductance result in **Figure IV.2** where break point is also seen in good agreement with surface tension (**Figure IV.1**).

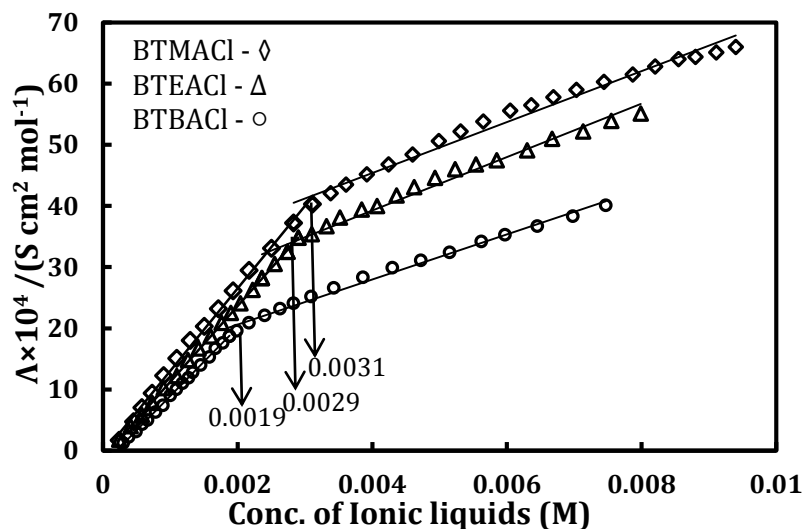


**Figure IV.2:** Plot of molar conductance ( $\Lambda$ ) with corresponding conc. (M) of ionic liquids.

**Table IV.2:** Free energy of micellization ( $\Delta G_{mic}$ ) and free energy of change ( $\Delta G$ ) obtained from degree of micelle ionization ( $\alpha$ ) and association constant ( $K_a$ ) of the solution ( $\beta$ -CD+ionic liquid) at 25°C evaluated from the conductance and surface tension measurement respectively.

Salt	$\alpha$	$\Delta G_{mic}$ (kJ/mol)	$K_a$	$\Delta G$ (kJ/mol)	$\beta$	$10^6 \Gamma_{max}$ (mol m <sup>-2</sup> )	$A_{min}$ (Å <sup>2</sup> )
$[(C_6H_5CH_2)N(CH_3)_3Cl]$	0.57	-16.29	$252.25 \pm 19$	19.14	0.43	2.37	70.19
$[(C_6H_5CH_2)N(C_2H_5)_3Cl]$	0.54	-16.56	$524.39 \pm 22$	18.17	0.46	2.28	72.67
$[(C_6H_5CH_2)N(C_4H_9)_3Cl]$	0.51	-16.83	$136.36 \pm 13$	17.44	0.49	2.13	77.88

### IV.3.2. Surface Tension

Surface tension ( $\gamma$ ) measurement gives significant indication about the formation of inclusion complex as well as stoichiometry of the host-guest assembly [17-20].

**Figure IV.3** illustrates the variations of surface tension ( $\gamma$ ) of 0.01M chosen three aforesaid ionic liquids with  $\beta$ -CD concentration at 298 K. The surface tension curves vary linearly with an addition of  $\beta$ -CD concentration to a maximum, and after then surface tension data not vary effectively with further adding of  $\beta$ -CD into the solutions. The linear

rising surface tension data demonstrates the decreasing tendency of the surface activity of the surface active ionic liquids. This is due to the fact that ionic liquids are encapsulated insight into the cavity of the  $\beta$ -CD and form the inclusion complexes (ICs) and loss their surface activity. The constant variation of surface tension after saturation point, make clear that the rest surface tension is only for the aqueous solutions of  $\beta$ -CD or pure water; because the inclusion complexes and aqueous solution of  $\beta$ -CD do not possess any surface activity [21]. The stoichiometry of the inclusion complexes has been obtained from concentration ratio of the ionic liquid and  $\beta$ -CD (IL: $\beta$ -CD) at the break point or the saturation point of the inclusion. From **Table IV.1** it has been seen that the concentration ratio of IL: $\beta$ -CD is 1:1.01, 1:1.02, and 1:1.05 for  $[(C_6H_5CH_2)N(CH_3)_3]Cl$ ,  $[(C_6H_5CH_2)N(C_2H_5)_3]$  and  $[(C_6H_5CH_2)N(C_4H_9)_3]Cl$  respectively, shows the 1:1 stoichiometric ratio of inclusion complex. From **Figure IV.4** it is found that the surface tension curves of the three selected ionic liquids in the presence of fixed amount (0.005M) of  $\beta$ -CD are higher than those in the absence of  $\beta$ -CD.

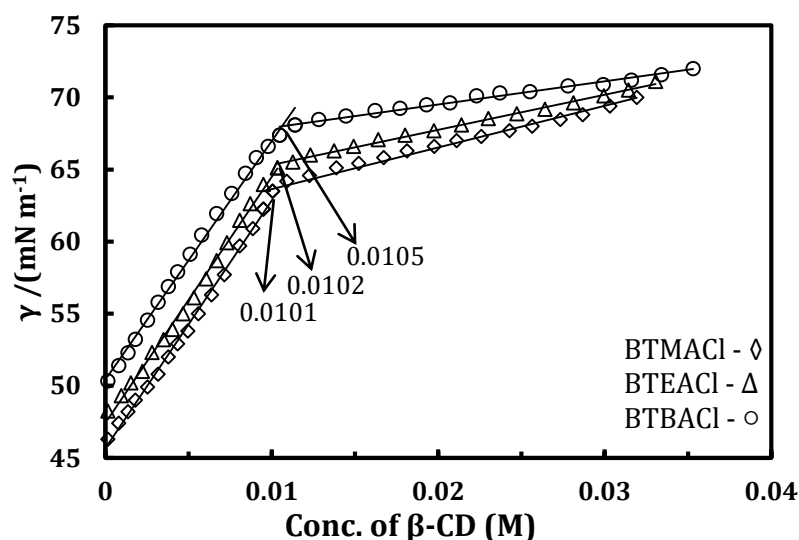


**Figure IV.3:** Plot of surface tension ( $\gamma$ ) of ionic liquids (0.01M) with corresponding conc. (M) of  $\beta$ -CD.

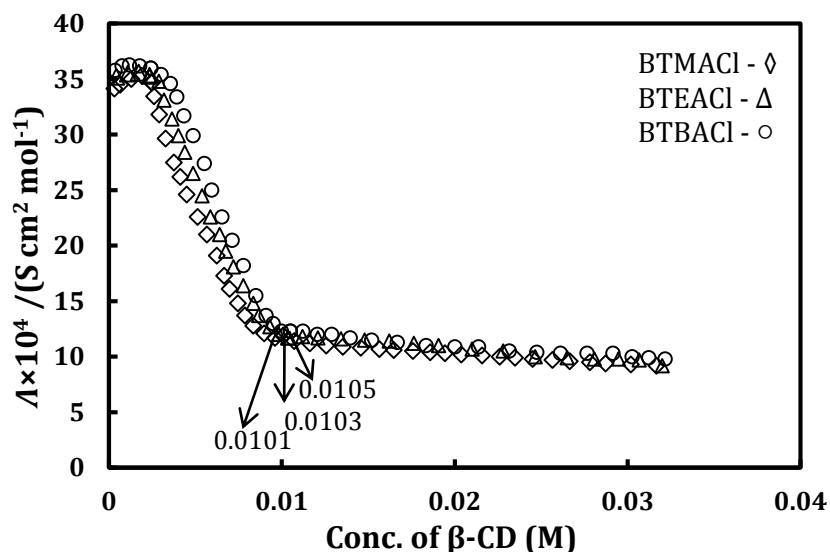


**Figure IV.4:** Plot of molar conductance ( $\Lambda$ ) of ionic liquids (0.01M) with corresponding conc. (M) of  $\beta$ -CD.

The concentration at which surface tension of ionic liquids (for fixed 0.005M  $\beta$ -CD) is almost constant is called as apparent critical micelle concentrations (CMC\*). The CMC\* 0.00499, 0.00503, and 0.00505 for  $[(C_6H_5CH_2)N(CH_3)_3Cl]$ ,  $[(C_6H_5CH_2)N(C_2H_5)_3Cl]$  and  $[(C_6H_5CH_2)N(C_4H_9)_3Cl]$  respectively, also suggested the 1:1 stoichiometric ratio of inclusion. Higher the CMC\* values caused by the presence of  $\beta$ -CD indicates that the formation of  $\beta$ -CD-ionic liquid inclusion complexes decreases the micelle formation ability of the ionic liquids. The surface tension values of each ionic liquid after the CMC in the presence of  $\beta$ -CD remain constant as that of the absence of  $\beta$ -CD. This also indicates that the inclusion complexes have no surface activity and that there is little interaction between the inclusion complexes and the micelles or the free surfactants.

### IV.3.3. Conductance

The shape of the curve (**Figure IV 5**) is quite similar to those generally obtained for an aqueous mixtures of ionic liquids and monomers of  $\beta$ -CD [22] as the concentration in  $\beta$ -CD cavities rises, the conductance of the mixture slightly increases, passes through a maximum, then decreases gradually, reach a minima, up to the saturation point (existence of a break in the curve) and then the change is constant even further addition



of  $\beta$ -CD into the solution systems. Such a behaviour denotes the formation of inclusion complexes between the ionic liquid molecules with the  $\beta$ -CD cavities.

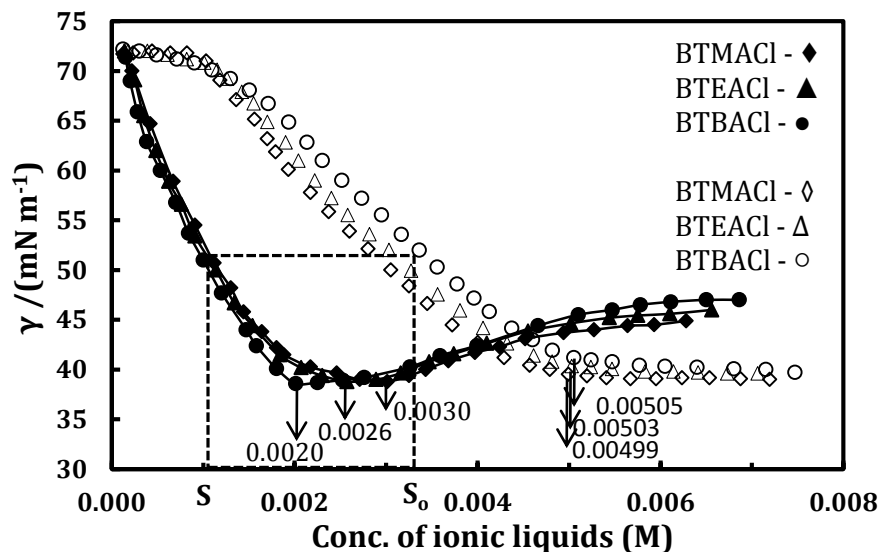
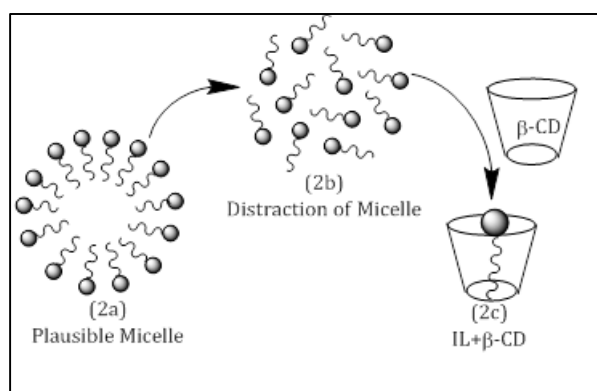


**Figure IV.5:** Plot of surface tension ( $\gamma$ ) with corresponding conc. of ionic liquids in absence (solid fill) and in presence (no fill) of  $\beta$ -CD.

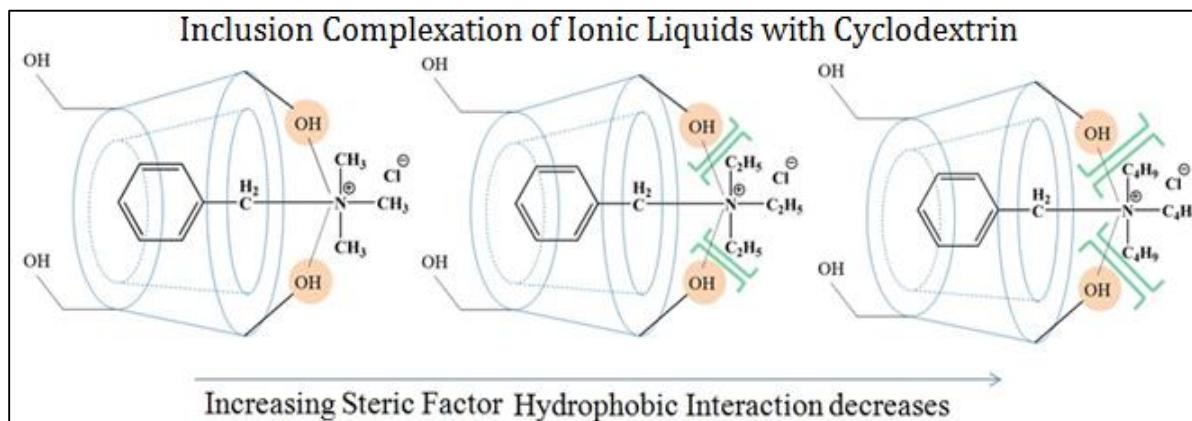
The initial increase of conductance at very low conc. of  $\beta$ -CD is ascribed to the progressive destruction of the micelles (**Scheme IV.2a**) of ionic liquids by inclusion of the benzyl group of ionic liquid into the  $\beta$ -CD cavities (i.e., the  $\beta$ -CD-ionic liquid interactions are stronger than those of the ionic liquid-ionic liquid interactions [23]). The destruction of the micelles is accompanied by a release of surfactant monomers and a release of counter ions initially linked to the surface of the micelles, which increases the conductance values.



**Scheme IV.2:** Schematic illustration of plausible micelle (2a), distraction of micelle (2b) and plausible inclusion formation (2c).

At the maximum of the conductance, micelles are supposed to have completely disappeared (**Scheme IV.2b**) and an excess of  $\beta$ -CD cavities reduces the quantity of free ionic liquids by formation of inclusion complexes (**Scheme IV.2c**), leading to a decrease of the conductance values. When most of the ionic liquid molecules are incorporated insight into the cyclodextrin cavities, a plateau of conductance is observed and its value is ascribed only to the charged inclusion complexes and to the counter ion  $\text{Cl}^-$ .

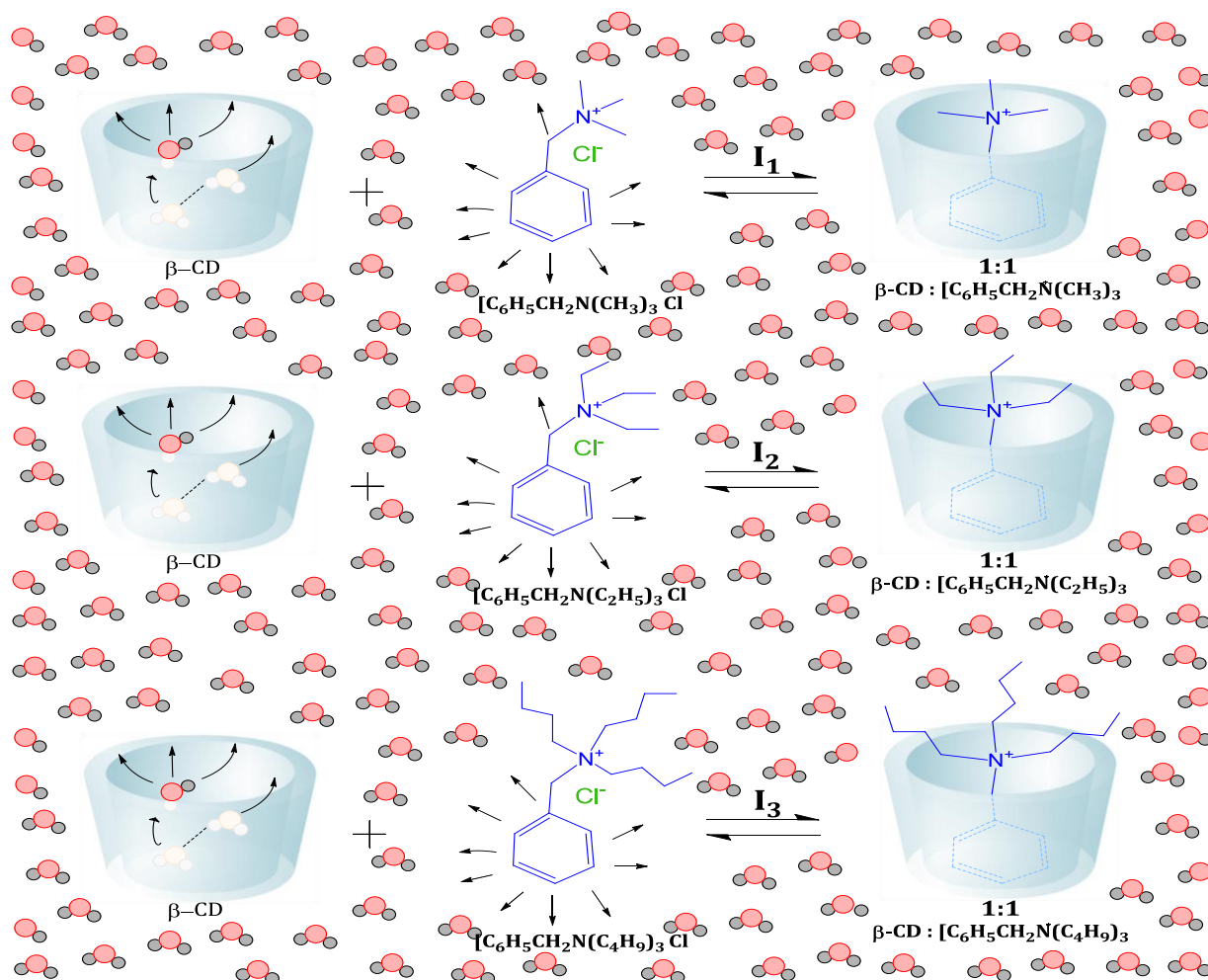
From output of the **Figure IV.5** and **Table IV.1**, the ratio of the  $\beta$ -CD concentration to the ionic liquid concentration at the saturation point or break point is equal to the 1.01, 1.03, and 1.05 for  $[(\text{C}_6\text{H}_5\text{CH}_2)\text{N}(\text{CH}_3)_3]\text{Cl}$ ,  $[(\text{C}_6\text{H}_5\text{CH}_2)\text{N}(\text{C}_2\text{H}_5)_3]\text{Cl}$  and  $[(\text{C}_6\text{H}_5\text{CH}_2)\text{N}(\text{C}_4\text{H}_9)_3]\text{Cl}$  respectively, has showed that  $\beta$ -CD-ionic liquid complexes are mainly formed with a 1:1 stoichiometry, i.e., only one molecule of ionic liquid encapsulated per  $\beta$ -CD cavity (**Scheme IV.3**).



**Scheme IV.3:** Schematic representation of mechanism of formation of inclusion complexes of cationic ionic liquids with  $\beta$ -cyclodextrin.

In the surface tension ( $\gamma$ ) study for the aforesaid three ionic liquids with  $\beta$ -CD shows single break point (**Figure IV.3**) in each  $\gamma$  vs. conc. curve, which clearly indicates  $\beta$ -CD can form 1:1 inclusion complexes with the hydrophobic benzyl moiety. The hydrophilic ammonium moiety or positive charge on the nitrogen atom remains hydrated at the outside of the cyclodextrin cavity and stabilized with oxygen atom of the

-OH group present in the rim of cyclodextrin (only in case of benzyltrimethylammonium chloride) (**Scheme IV.4**).



**Scheme IV.4:** Schematic representation of inclusion complexes of cationic ionic liquids with  $\beta$ -cyclodextrin.

#### IV.3.4. $^1\text{H}$ NMR

Inclusion of a guest molecule into the cavity of  $\beta$ -cyclodextrin has been studied by the upfield chemical shift of the protons of cyclodextrin molecule in  $^1\text{H}$  NMR spectra. According to the  $^1\text{H}$  NMR study in the molecular structure of  $\beta$ -cyclodextrin the H3 and H5 hydrogen's are situated inside the conical cavity, mainly, the H3 are placed near the wider rim whereas H5 are placed near the narrower rim, the other H1, H2 and H4

hydrogens are situated at the exterior of the cyclodextrin molecule (**Figure IV.6**). Since the H3 is located near the wider rim of CD, through which the guest enters, the shift is higher for it than the H5 proton [24].

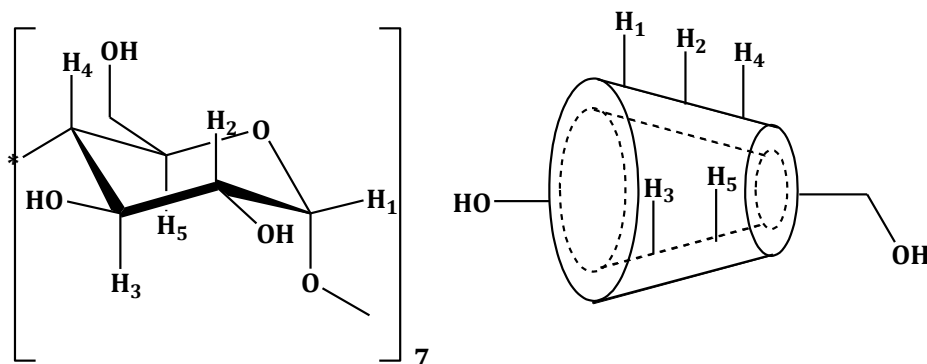


**Figure IV.6:** (a) Stereo-chemical configuration, (b) truncated conical structure of  $\beta$ -cyclodextrin with interior and exterior protons.

The other H1, H2 and H4 hydrogen's also show reasonable upfield chemical shift, but it is less compared to that of the interior protons [25-27]. Here, the inclusion phenomenon of chosen benzyltrialkylammonium chloride  $[(C_6H_5CH_2)N(C_nH_{2n+1})_3Cl]$ ; where  $n=1,2,4$ ] with  $\beta$ -CD have been studied by  $^1H$  NMR spectra by taking 1:1 molar ratio in  $D_2O$  (**Figure IV.7-9**).

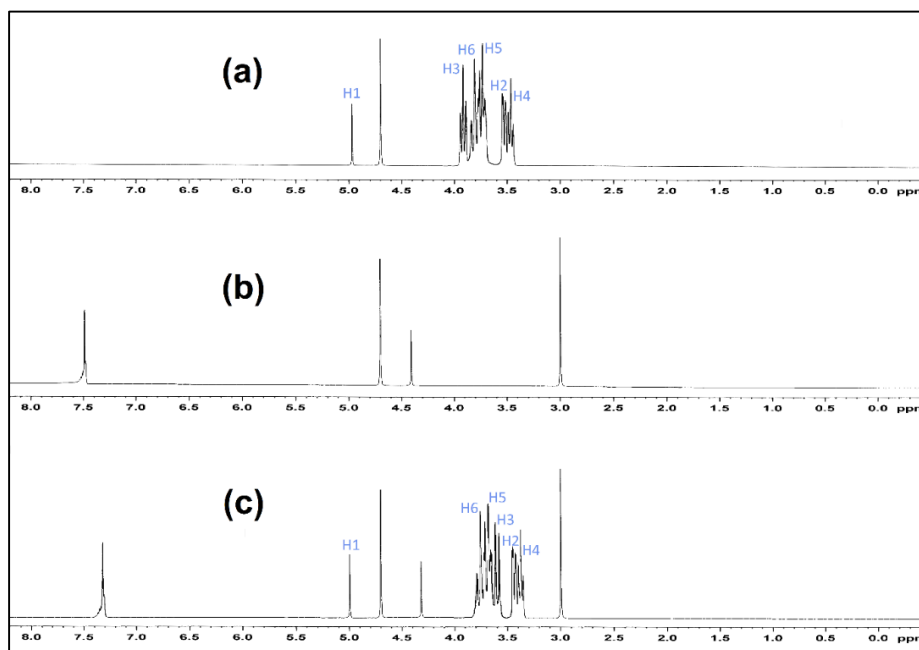


**Figure IV.7:**  $^1H$  NMR spectra of (a)  $\beta$ -CD, (b)  $[(C_6H_5CH_2)N(CH_3)_3]Cl$ , and (c) inclusion complex.

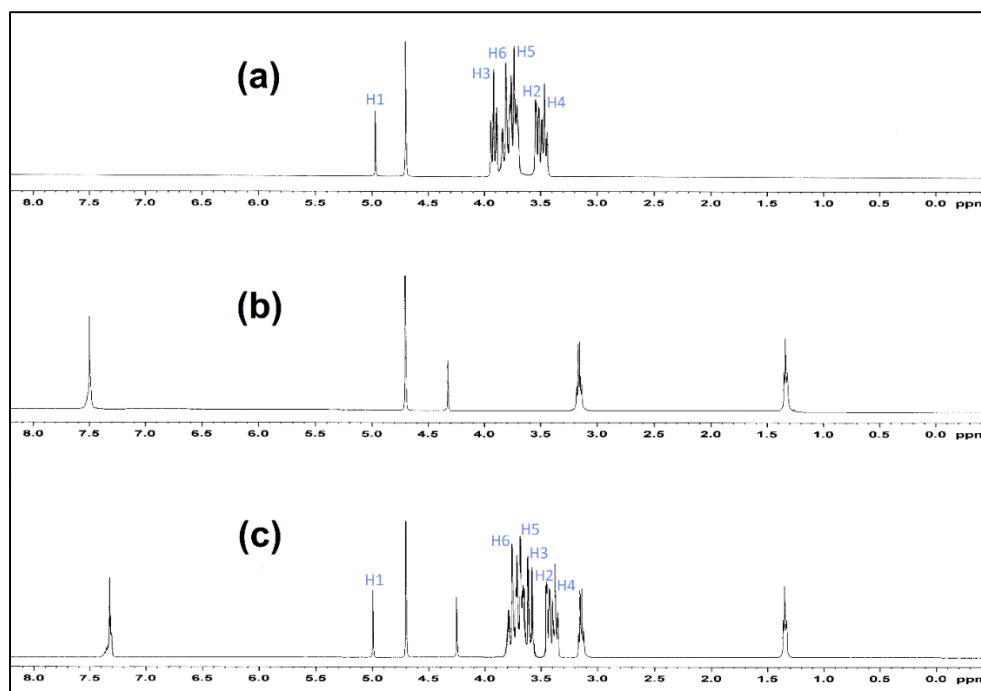


**Figure IV.8:**  $^1\text{H}$  NMR spectra of (a)  $\beta$ -CD, (b)  $[(\text{C}_6\text{H}_5\text{CH}_2)\text{N}(\text{C}_2\text{H}_5)_3]\text{Cl}$ , and (c) inclusion complex.

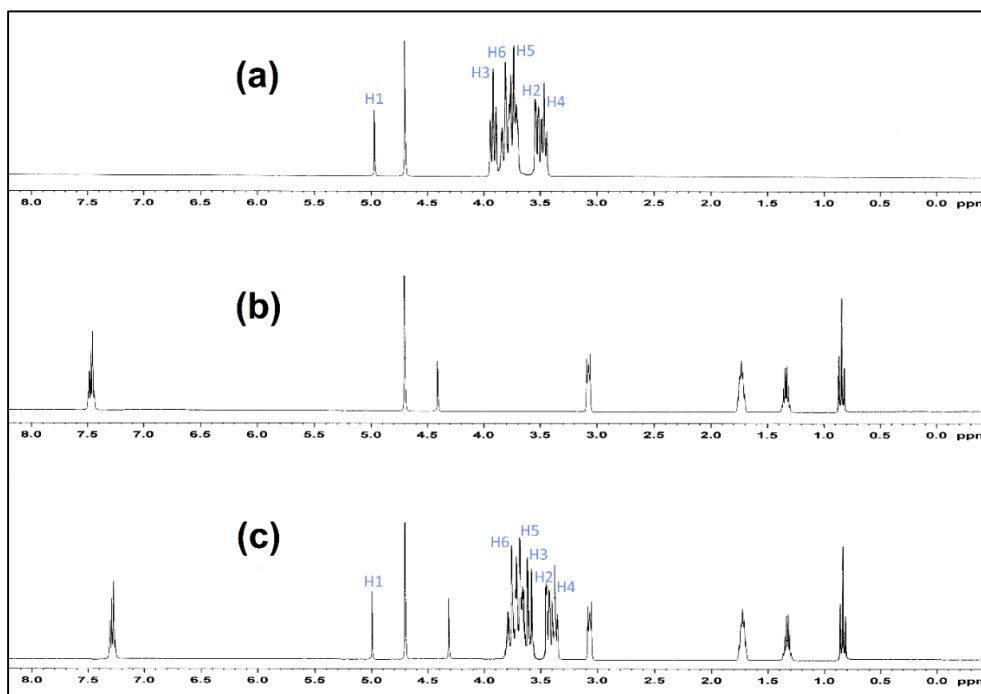


**Figure IV.9:**  $^1\text{H}$  NMR spectra of (a)  $\beta$ -CD, (b)  $[(\text{C}_6\text{H}_5\text{CH}_2)\text{N}(\text{C}_4\text{H}_9)_3]\text{Cl}$ , and (c) inclusion complex.

It has been found that there are considerable upfield shifts of interior H3 and H5 protons, as well as that of the interacting protons i.e., aromatic and methylene protons of the benzyl group of benzyltrialkylammonium cations [28]. This establishes that inclusion phenomenon has occurred between the chosen ionic liquid with cavity of the  $\beta$ -CD molecule [29, 30].

### IV.3.5. Association Constant and Other thermodynamic properties

The association constants for 1:1 inclusion complexes of  $\beta$ -CD and ionic liquid was determined from the surface tension measurements by using the numerical method developed by Lu et al. [21]. We have used two surface tension curves in **Figure IV.5** (with and without  $\beta$ -CD) to determine the value of association constant, which allows justification of the assumption made. The plot of  $S_0 - [S]$  vs  $\left(\frac{S_0}{[S]} - 1\right)$  shown in **Figure IV.10** gives the slope  $\left(-\frac{1}{K_a}\right)$ , and thus the association constants ( $K_a$ ) for the inclusion complexes of  $\beta$ -CD-ionic liquids<sup>16</sup> and free energy change ( $\Delta G$ ) are determined, and listed in **Table IV.2**.

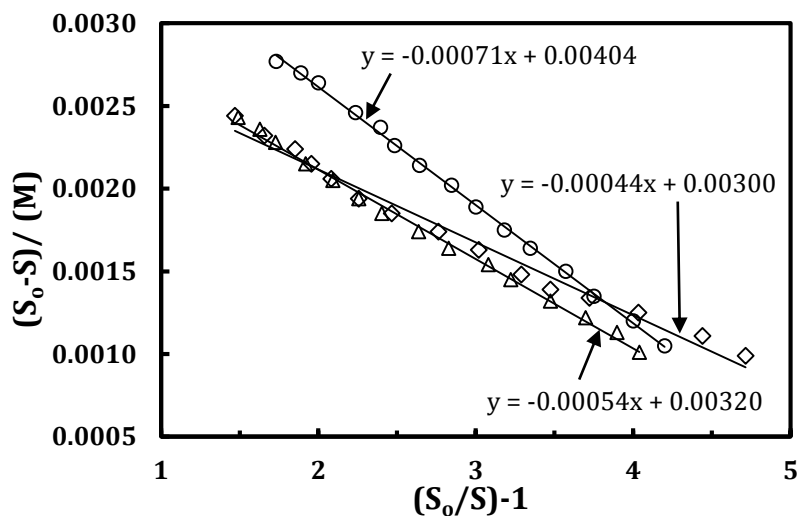


**Figure IV.10:** Relationship between  $(S_0 - S)$  and  $(S_0/S) - 1$  for solution of ionic liquids along and mixed with  $\beta$ -CD.

Free energy of micellization ( $\Delta G_{mic}$ ), degree of micellization ( $\theta$ ) and degree of counterion binding ( $\phi$ ) evaluated from the conductance; association constant ( $K_a$ ), free energy of change ( $\Delta G$ ),  $\Gamma_{max}$ , and  $A_{min}$  obtained from surface tension of the solution ( $\beta$ -

CD+ionic liquid) at 25°C respectively (**Table IV.2**). The degree of micelle ionization ( $\theta$ ) was calculated by taking the ratio between the slopes of the linear portions above and below the break point in the conductivity profiles. The larger value of  $\theta$  for the complex micelles is indication of an increased degree of ionic dissociation (**Table IV.2**) as a result of the interaction of ionic liquids with  $\beta$ -CD. The free energy of micellization ( $\Delta G_{mic}$ ) can be calculated using the equation of [31]

$$\Delta G_{mic} = RT(2-\theta)\ln CMC$$

The negative  $\Delta G_{mic}$  values (**Table IV.2**) indicates that the presence of  $\beta$ -CD makes the process feasible and can be explained on the basis that more  $\beta$ -CD will be able to encapsulate more monomers and the amount of ionic liquids needed to form the micelle will obviously disappeared. The degree of counter ions binding ( $\phi$ ) onto the self-aggregated assemblies was obtained from the slopes of the  $\Lambda$  vs  $[(C_6H_5CH_2)N(C_nH_{2n+1})_3]Cl$  isotherm in the pre-micellar region ( $S_1$ ) and the post-micellar region ( $S_2$ ) using the following relationship:

$$\phi = 1 - \frac{S_2}{S_1}$$

The  $\phi$  factor includes the fraction of free energy required to condense the counter ions on the aggregate to reduce the repulsion between the adjacent monomer head groups [32].

From the perusal of **Table IV.2** it is clear that the association constants ( $K_a$ ) for benzyltrimethylammonium chloride is higher compared to the other two ionic liquids; is obviously due to the fact of steric factor of the side chain group of cationic part of the chosen ionic liquids. The higher the side chain group increases the steric hindrance effect, i.e., butyl group in  $[(C_6H_5CH_2)N(C_4H_9)_3]Cl$  is more steric effect than ethyl group in  $[(C_6H_5CH_2)N(C_2H_5)_3]Cl$ , which is in turn more than methyl group in  $[(C_6H_5CH_2)N(CH_3)_3]Cl$  (**Scheme IV.4**); which clearly state the benzyl group of benzyltrimethylammonium cationic part of the ionic liquid is more associated/encapsulated with  $\beta$ -CD (**Scheme IV.4**). On other hand more negative  $\Delta G$  for  $[(C_6H_5CH_2)N(CH_3)_3]Cl$  than the rest two is also undoubtedly speak out that benzyltrimethylammonium charge or cationic part of the ionic liquid is more feasibly associated.

The maximum surface excess concentration ( $\Gamma_{\max}$ ), and the minimum area of exclusion per molecule at the air-solution interface ( $A_{\min}$ ) were estimated for the three surface active ionic liquids to the slope of the tensiometric profile near the CMC, is quantified by applying the Gibbs adsorption isotherm [33]. The values of  $\Gamma_{\max}$  and  $A_{\min}$  are also listed in **Table IV.2**. The increase in the  $A_{\min}$  values with temperature may be ascribed to the greater kinetic motion of the monomers populating the air-solution interface. It was noticed from **Table IV.2** that the values of  $\Gamma_{\max}$  decrease and those of  $A_{\min}$  increase, with the increase of alkyl chain length; which means the ionic liquid molecules with the short alkyl chain (i.e., trimethyl group) can make packing more closely or arrange more tightly than longer one.

#### IV.4. CONCLUSIONS

The surface tension, conductance and NMR study gives the clear indication of 1:1 host-guest inclusion complex formation of a series of surface active ionic liquids, benzyltrialkylammonium chloride  $[(C_6H_5CH_2)N(C_nH_{2n+1})_3Cl]$ ; where  $n=1,2,4$  ] with aq.  $\beta$ -cyclodextrin. The study also expose that benzyl, the hydrophobic group of ionic liquids encapsulated insight into the cavity of  $\beta$ -cyclodextrin and form the inclusion complex. This study also demonstrated that hydrophobic interactions and hydrogen bonding contribute to the inclusion of ionic liquids in CDs. It was found that addition of  $\beta$ -CD causes the shifting of micellization of the ionic liquids towards the higher concentration. This indicates the inclusion complex formation between the ionic liquids and  $\beta$ -CD.



# CHAPTER-V

## **PROBING INCLUSION COMPLEX FORMATION OF AMANTADINE HYDROCHLORIDE WITH 18-CROWN-6 IN METHANOL BY PHYSICOCHEMICAL APPROACH**

### **V.1. INTRODUCTION**

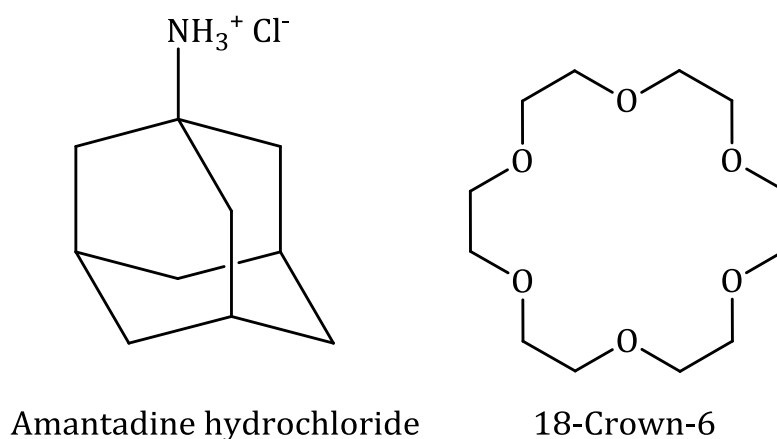
Host-guest interaction has been termed 'a complementary stereo-electronic arrangement of binding sites in host and guest' [1]. In the chemical sense the host is usually an organic molecule containing specific receptor sites while the guest is normally a metal or organic cation. Host-guest interactions have recognized importance in many biological processes, including enzyme catalysis and inhibition, antibody-antigen interactions, and membrane transport. A particularly fruitful field of organic synthesis during the past several years has been the design and preparation of macrocyclic molecules of the cyclic polyether type with the intent to mimic certain biological host-guest interactions [1-4]. Several workers have reported the attachment of organic ammonium [5] groups to hosts which are analogues of 18-crown-6 with the subsequent enhancement of a reaction between host and guest components away from the site of primary binding.

The crown ethers were of a great interest since their discovery had been reported by Pedersen in 1967 [6]. The ability of these macrocycles to form non-covalent, H-bonding complexes with ammonium cations has been actively investigated with an eye toward biological applications [7,8], molecular recognition [9,10], self-assembly [11,12], crystal engineering [13,14], and catalysis [15]. The stoichiometry and stability of these host-guest complexes depend both on the size of the crown ether and on the nature of the ammonium cation ( $\text{NH}_4^+$ ,  $\text{RNH}_3^+$  etc) [16,17]. The numerous studies of 18-crown-6 (18C6) and its derivatives, which have the highest affinity for ammonium cations, invariably showed a 1:1 stoichiometry with both  $\text{NH}_4^+$  and  $\text{RNH}_3^+$  cations in solution [18] and in the solid state [19,20].

Crown ether-ammonium complexes are of fundamental interest as prototypical systems involving multiple hydrogen bonds. Study of these simple multiply-bound complexes is a promising means of gaining insight into much more complex

macromolecular systems, such as those involved in protein folding or in the pairing of nucleobases in polynucleic acids [21]. Host parameters of importance in binding both metals and organic ammonium cations include cavity size, donor atom number and type, ring number and type, ring substituents, and ring conformation. Guest parameters for organic ammonium cations differ from those of metal cations because of the different binding mechanisms involved for the two types of guest. Metal cations are sequestered within the macrocyclic ring, whereas ammonium cations hydrogen bond to the ring donor atoms. Thus, guest parameters significant to organic ammonium cation binding include number of hydrogen atoms available for hydrogen bonding.

Amantadine (**Scheme V.1**) is tricyclic aminohydrocarbons with antiviral activity directed uniquely against influenza A virus. The compounds have a potential to inhibit the early phases of viral replication by preventing uncoating of the viral genome and virus-mediated membrane fusion. The drug is used in the prevention and treatment of influenza A infections [22, 23].



**Scheme V.1:** Molecular structure of Amantadine hydrochloride and 18C6.

On the other hand, macrocyclic [24] and macrobicyclic polyethers [25] have been extensively used as interesting model compounds for the study of molecular effect on membrane permeability [26,27], due to their many similarities to cyclic antibiotics and biological transport agents. Considerable attention has been focused on the interactions between different protonated amines and macrocyclic ligands in order to study the molecular effect on membrane permeability [28-30].

One interesting property of crown ethers is that the electron pairs present in the ring heteroatoms provide the molecule with the ability to complex a wide range of cations in the empty cavity present in the centre of the ring [31]. A space filling model of 18-crown-6 is shown in **Figure V.1** illustrating the central cavity in which  $K^+$  ions bind by coordinating to the six surrounding ether oxygen atoms. In the case of 18-crown-6, the diameter of the interior hole is about 4.0 Å [31]. That structural feature allows for crown ethers to form a number of complexes with cationic species [32].

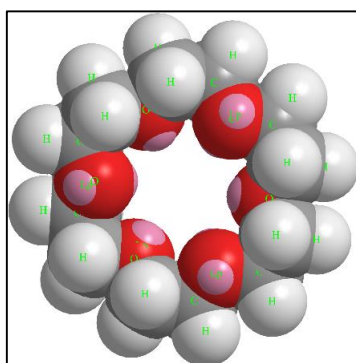


**Figure V.1:** A space filling model of 18-crown-6 showing the open space at the center of the crown and electron pairs present on the exposed oxygen atoms (in pink).

Conductance measurements as a sensitive and powerful technique to study the complexation of macrocyclic ligands with different cations in a variety of non-aqueous and mixed solvents [33,34]. The thermodynamics of complexation of amantadine ion with different crown ethers and cryptands in acetonitrile solvents have been reported in the literature [35]. In this paper a conductance study, surface tension study and density study of the complex formed between amantadine hydrochloride (ADH) and 18-crown-6 (18C6) in methanol solution was reported and discuss the influence of several structural and medium parameters on the complexation reaction. The structure of the crown ether is shown in **Scheme V.1**.

## V.2. EXPERIMENTAL SECTION

### V.2.1 Reagents

The Amantadine hydrochloride (ADH) and 18-crown-6(18C6) of puriss grade were bought from Sigma-Aldrich, Germany and used as purchased. The mass fraction purity of ADH and 18C6 were  $\geq 0.99$  and 0.98 respectively.

## V.2. 2. Instrumentations

Prior to the start of the experimental work solubility of the chosen crown ether in methanol and ADH in methanolic solution of 18C6 have been precisely checked and observed that the drug molecule ADH freely soluble in all proportion of methanolic 18C6 solution. All the stock solutions of the drug molecule were prepared by mass (weighed by Mettler Toledo AG-285 with uncertainty 0.0003g), and then the working solutions were obtained by mass dilution at 298.15 K. The conversions of molarity into molality have been done [36] using density values. Adequate precautions were made to reduce evaporation losses during mixing.

The surface tension experiments were done by platinum ring detachment method using a Tensiometer (K9, KRÜSS; Germany) at the experimental temperature. The accuracy of the measurement was within  $\pm 0.1 \text{ mN}\cdot\text{m}^{-1}$ . Temperature of the system was maintained at 298.15 K by using Omniset thermostat having uncertainty in temperature  $\pm 0.01 \text{ K}$ .

The conductance values were obtained by using Systronics-308 [37]. The study was carried out using Brookfield TC-550 water bath with thermostat maintaining at the experimental temperatures having uncertainty of  $\pm 0.01 \text{ K}$ .

The densities ( $\rho$ ) of the solvents were measured by means of vibrating *U*-tube Anton Paar digital density meter (DMA 4500M) with a precision of  $\pm 0.00005 \text{ gcm}^{-3}$  maintained at  $\pm 0.01 \text{ K}$  of the desired temperature. It was calibrated by passing triply distilled, degassed water and dry air.

Infrared spectra were recorded in 8300 FT-IR spectrometer (Shimadzu, Japan). The details of the instrument have formerly been described [38].

## V.3. RESULTS AND DISCUSSION

### V.3.1. Conductance

The molar conductance ( $\Lambda$ ) of ADH ( $5 \times 10^{-4} \text{ M}$ ) in methanol solution was monitored as a function of crown ether to amantadine ion mole ratio at various temperatures [Table V.1]. The resulting molar conductance vs. crown/cation mole ratio plots at 298.15, 303.15, and 308.15 K are shown in Figure V.2. In every case, there is a gradual decrease in the molar conductance with an increase in the crown ether concentration. This behavior indicates that the complexed amantadine ion is less mobile than the corresponding amantadine ion in methanol. As can be seen from

**Figures V.2**, the complexation of amantadine ion with 18C6, addition of the crown solution to the amantadine solution causes a continuous decrease in the molar conductance, which begins to level off at a mole ratio greater than one, indicating the formation of a stable 1:1 complex [39, 40]. By comparison of the molar conductance-mole ratio plot for amantadine ion -18C6 systems obtained at different temperatures (**Figure V.2**), it can be observed, that the corresponding molar conductance increased rapidly with temperature, due to the decreased viscosity of the solvent and, consequently, the enhanced mobility of the charged species present.

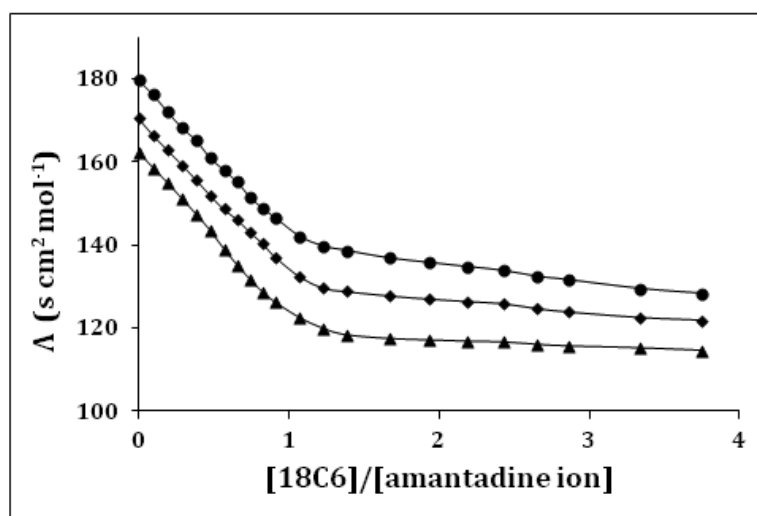


**Figure V.2:** Molar conductance vs  $[18C6]/[amantadine\ ion]$  at 298.15 K (▲), 303.15 K (◆), 308.15 K (●).

**Table V.1:** Values of observed molar conductivities ( $\Lambda$ ) at various mole ratios for the system Amantadine-18C6 at different temperature.

Mole Ratio	Conductance ( $\Lambda$ ) ( $S. cm^2. mol^{-1}$ )		
	293.15 K	298.15 K	303.15 K
0	162.40	170.60	179.74
0.099	158.46	166.42	176.18
0.196	154.84	162.80	172.00
0.291	151.06	159.32	168.20
0.385	147.32	155.68	165.16
0.476	143.50	152.02	161.00
0.566	139.12	148.68	158.16

---

0.654	135.24	146.20	155.24
0.740	131.68	143.12	151.56
0.825	128.58	140.34	148.82
0.909	126.20	137.10	146.60
1.071	122.46	132.38	142.12
1.228	119.88	129.60	139.76
1.379	118.34	128.82	138.72
1.667	117.44	127.76	136.88
1.935	117.10	127.00	135.80
2.187	116.80	126.42	134.80
2.424	116.62	125.90	133.90
2.647	116.04	124.72	132.48
2.857	115.66	123.92	131.64
3.333	115.20	122.60	129.52
3.750	114.58	121.94	128.34

---

### V.3.2. Association constant and Thermodynamic parameter

The 1: 1 complexation of amantadine ion with 18C6 crown ether can be expressed by the following equilibrium



The corresponding equilibrium constant,  $K_f$  is given by

$$K_f = \frac{[MC^+]}{[M^+][C]} \times \frac{f(MC^+)}{f(M^+)f(C)} \quad (2)$$

where  $[MC^+]$ ,  $[M^+]$ ,  $[C]$  and  $f$  represent the equilibrium molar concentrations of the complex, free cation, free ligand and the activity coefficients of the species indicated, respectively. Under the dilute conditions used, the activity coefficient of uncharged macrocycle,  $f(C)$ , can be reasonably assumed as unity [41]. The use of the Debye-Hückel limiting law [42], leads to the conclusion that  $f(M^+) \sim f(MC^+)$ , so the activity coefficients in Equation (2) cancel. The complex formation constant can be expressed in terms of the molar conductances,  $\Lambda$ , by the following equations [39, 41].

$$K_f = \frac{[MC^+]}{[M^+][C]} = \frac{(\Lambda_M - \Lambda_{obs})}{(\Lambda_{obs} - \Lambda_{MC})[C]} \quad (3)$$

$$\text{Where } [C] = C_C - \frac{C_M(\Lambda_M - \Lambda_{obs})}{(\Lambda_M - \Lambda_{MC})} \quad (4)$$

Here,  $\Lambda_M$  is the molar conductance of the metal ion before addition of ligand,  $\Lambda_{MC}$  the molar conductance of the complexed ion,  $\Lambda_{obs}$  the molar conductance of the solution during titration,  $C_C$  the analytical concentration of the macrocycle added and  $C_M$  the analytical concentration of the salt. The complex formation constant,  $K_f$ , and the molar conductance of the complex,  $\Lambda_{MC}$ , were evaluated by using Equations (3) and (4).

In order to have a better understanding of the thermodynamics of the complexation reactions of amantadine ion with the 18C6 crown ether it is useful to consider the enthalpic and entropic contributions to these reactions. The  $\Delta H^\circ$  and  $\Delta S^\circ$  values for the complexation reactions were evaluated from the corresponding  $\log K_f$  and temperature data by applying a linear least-squares analysis according to the equation:

$$2.303 \log K_f = -\frac{\Delta H^\circ}{RT} + \frac{\Delta S^\circ}{R} \quad (5)$$

Plots of  $\log K_f$  vs.  $\frac{1}{T}$  for Amantadine -18C6 complex is linear (**Figure V.3**).

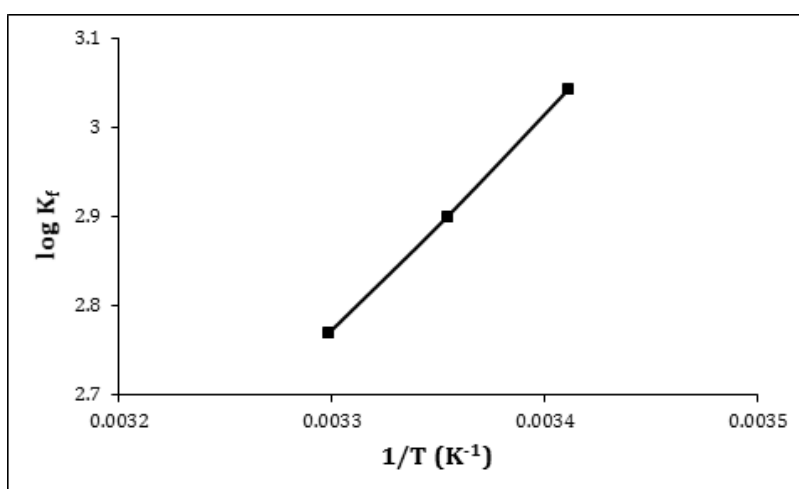


**Figure V.3:** The linear relationship of  $\log K_f$  vs  $1/T$  for the interaction between amantadine hydrochloride with 18C6.

The enthalpy ( $\Delta H^\circ$ ) and entropy ( $\Delta S^\circ$ ) of complexation were determined in the usual manner from the slopes and intercepts of the plots and the results are also included in **Table V.2**. Both of these two parameters have negative values. The negative values of enthalpy confirm that when ADH interact with the crown ether molecules the overall energy of the system is decreased, i.e., there is some stabilization interaction in the system, whereas negative values of entropy factor indicate that there is an ordered arrangement, i.e., complex formation takes place between the ADH and the 18C6 molecule. The negative value of entropy is unfavourable for the spontaneity of the complex formation, but this effect is overcome by higher negative value of  $\Delta H^\circ$ . The values of  $\Delta G^\circ$  (**Table V.2**) for the complex formation was found negative suggesting that the complex formation process proceeds spontaneously. The data shown in table indicates that formation constant  $\log K_f$  for amantadine ion with 18C6 is highest at 298.15 K and decreases with increase in temperature i.e. amantadine ion form stable complex with 18C6 at 298.15K.

**Table V.2:** Values of formation constant, enthalpy, entropy and free energy change of amantadine-18C6 complex in methanol solution.

Cation	Crown	Log $K_f$			$\Delta H^\circ$ (kJ mol <sup>-1</sup> )	$\Delta S^\circ$ (J mol <sup>-1</sup> K <sup>-1</sup> )	$\Delta G^\circ$ (kJ mol <sup>-1</sup> )
		298.15K	303.15K	308.15K			
Amantadine	18C6	3.04	2.90	2.77	-46.56	-100.58	-16.57

### V.3.3. Surface tension

Surface tension ( $\gamma$ ) measurement provides significant indication about formation of inclusion complex as well as stoichiometry of the host-guest assembly [43-45]. The values of surface tension at different concentration of 18C6 are listed in **Table V.3**.

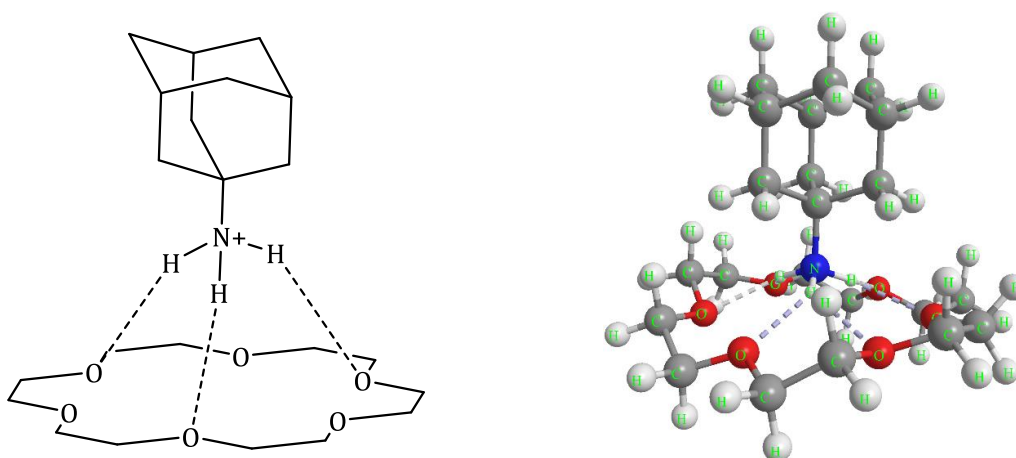


**Table V.3:** Experimental values of surface tension ( $\gamma$ ) corresponding to concentration of 18C6 in methanolic solution.

Conc. of 18C6 (mM)	Surface tension ( $\gamma$ ) (mN.m <sup>-1</sup> )
0.00	26.5
0.91	25.8
1.67	25.2
2.31	24.7
2.86	24.1
3.33	23.7
3.75	23.3
4.12	22.9
4.44	22.5
4.74	22.2
5.00	21.9
5.24	21.8
5.45	21.7
5.65	21.7
5.83	21.6
6.00	21.6
6.15	21.5
6.30	21.5
6.43	21.4
6.55	21.4
6.67	21.4

In the present work ADH have a hydrophobic group and a terminal  $-\text{NH}_3^+$  group (**Scheme V.1**) due to which ADH shows surfactant like activities, thus  $\gamma$  of the ADH solution shows decreasing trend. In this work when 18C6 was added in ADH solution the proton of the  $-\text{NH}_3^+$  group binds to the alternate three oxygen atom of the crown ether and the formation of three H-bonds occurs (**Scheme V.2**). As a result charged portion of the amantadine ion form complex with 18C6 and due to the formation of complex effect of hydrophobic portion increases i.e. surface tension of the solution

again decreases slowly. At a certain conc. of ADH and crown ether, a single break was observed in the surface tension curve (**Figure V.4**).



**Scheme V.2:** Schematic presentation of complexation between amantadine ion and 18C6 and corresponding energy minimized structure of the complex.

The break point in surface tension curve not only indicates the formation of complex between amantadine ion and 18C6 but also about its stoichiometry, i.e., appearance of single break point in the plot indicates 1:1 stoichiometry of the complex. The value of  $\gamma$  at the break point and corresponding concentration of crown ether have been listed in **Table V.4**. Hence the plausibility of formation of complex can be predicted from surface tension study.

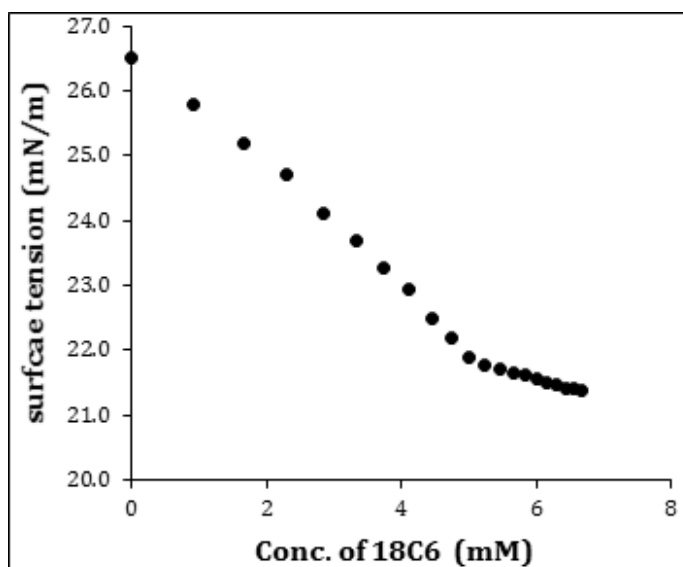


**Figure V.4:** Variation of surface tension of amantadine with increasing concentration of 18C6 at 298.15 K.

**Table V.4:** Values of surface tension ( $\gamma$ ) at the break point with corresponding to concentration of 18C6 in methanolic solution at 298.15 K.

Conc. (mM)	$\gamma$ (mN.m <sup>-1</sup> )
5.07	21.99

### V.3.4. IR Study

FTIR spectra of the complex, 18C6 and that of pure ADH were obtained in the region 400-4000 cm<sup>-1</sup>. If the FTIR spectrum of 18C6 was compared with that of complex, it was noticed that the peaks observed in pure 18C6 (**Figure V.5**) at 1120 cm<sup>-1</sup> correspond to COC group shift to 1106 cm<sup>-1</sup> in the complex (**Figure V.5**). The frequency of the C-O-C asymmetric stretching vibrations of a polyether,  $\nu_{as}$  (COC), decreases upon interaction of the O atoms with the protons of the ammonium group via hydrogen H bonds. The N-H stretching band of the ammonium group expected for amantadine ion in the region 2961 to 3087 cm<sup>-1</sup> by Pierre D. Harvey [46] was observed in pure ADH at 3047 cm<sup>-1</sup>. This peak shifts to 3027 cm<sup>-1</sup> revealed that the N-H bonds were involved in the complex formation. The characteristic peak of ADH at 2927 cm<sup>-1</sup> was shifted to 2909 cm<sup>-1</sup> in the complex. The peak at 1086 cm<sup>-1</sup> corresponding to C-N bend of the C-N bond of ADH shifts to higher frequencies [47]. Thus it may be concluded that amantadine was strongly bound to 18C6 through H-bonds of the ammonium group.

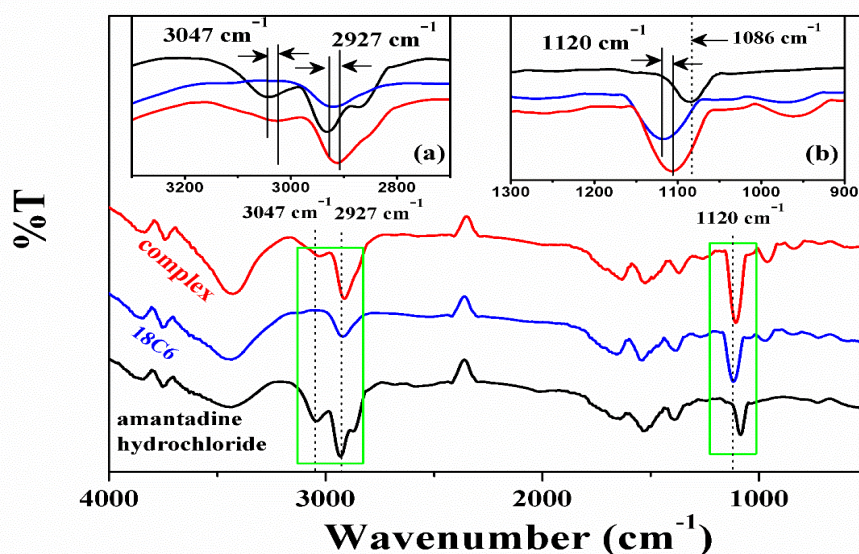


**Figure V.5:** FTIR spectra of pure amantadine hydrochloride (black), 18-crown-6 (blue) and complex (red).

### V.3.5. Apparent molar volume

The characteristic behavior of interaction present in complex of solute has also been obtained from apparent molar volume. The sum of the geometric volume of the central solute molecule and changes in the solvent volume due to its interaction with the solute around the co-sphere is the measure of apparent molar volume. The physical properties of binary mixtures in different mass fractions ( $w_1=0.001, 0.004, 0.007$ ) of methanolic 18C6 solutions at 298.15, 303.15, 308.15 K are reported in **Table V.5**. Here  $\phi_v$  has been determined from the measured density of the solutions at 298.15 K, 303.15 K, 308.15 K (**Table V.6**) and by using the suitable equation.  $\phi_v$  varies linearly with the square root of molal concentration and is fitted to the Masson equation, from where the limiting apparent molar volume ( $\phi_v^0$ ) has been determined (**Table V.7**) [48]. The limiting molar volume ( $\phi_v^0$ ) signify the solute-solvent interactions in the amantadine + 18C6 ternary solution systems. The magnitude of which is found to be positive for all the systems under study, indicating strong solute-solvent interactions [44,49].

**Table V.5:** Experimental values of density ( $\rho$ ) in different mass fraction of methanolic solution of 18C6.

Solvent mixture	Temp (K)	$\rho \cdot 10^{-3}$ (kg·m <sup>-3</sup> )
$w_1=0.001$	298.15	0.79378
	303.15	0.79141
	308.15	0.78899
$w_1=0.004$	298.15	0.79540
	303.15	0.79207
	308.15	0.78962
$w_1=0.007$	298.15	0.79627
	303.15	0.79336
	308.15	0.78107

**Table V.6:** Experimental values of densities ( $\rho$ ) corresponding to concentration in different mass fractions of methanolic solution of 18C6 at different temperature.

Concentration (M)	$\rho \cdot 10^{-3}$ ( $\text{kg} \cdot \text{m}^{-3}$ )		
	298.15 K	303.15 K	308.15 K
<b>W<sub>1</sub> = 0.001</b>			
0.002	0.79392	0.79156	0.78914
0.004	0.79407	0.79172	0.78930
0.006	0.79423	0.79188	0.78947
0.008	0.79440	0.79205	0.78965
<b>W<sub>1</sub> = 0.004</b>			
0.002	0.79552	0.79221	0.78977
0.004	0.79566	0.79236	0.78994
0.006	0.79581	0.79252	0.79012
0.008	0.79597	0.79270	0.79029
<b>W<sub>1</sub> = 0.007</b>			
0.002	0.79638	0.79348	0.79121
0.004	0.79651	0.79362	0.79137
0.006	0.79666	0.79377	0.79154
0.008	0.79681	0.79394	0.79172

**Table V.7:** Limiting apparent molar volume ( $\phi_v^0$ ) and experimental slope ( $S_v^*$ ) in different mass fractions of methanolic solution of 18-crown-6.

Temp.(K)	$\phi_v^0 \times 10^6$ ( $\text{m}^3 \cdot \text{mol}^{-1}$ )	$S_v^* \times 10^6$ ( $\text{m}^3 \cdot \text{mol}^{-3/2} \cdot \text{kg}^{1/2}$ )
<b>W<sub>1</sub>=0.001</b>		
298.15	156.91	-174.98
303.15	152.32	-162.19
308.15	148.11	-139.57
<b>W<sub>1</sub>=0.004</b>		
298.15	174.48	-280.76
303.15	164.06	-254.20
308.15	153.75	226.20

	$W_1=0.007$	
298.15	181.95	-311.69
303.15	175.74	-294.20
308.15	163.04	-284.41

The plot of  $\phi_v^\circ$  values against different temperature at different mass fractions are represented in **Figure V.6**, which suggests that  $\phi_v^\circ$  values increases with increase of mass fraction at same temperature and decreases with increasing the temperature. The values of  $\phi_v^\circ$  increases with the increase of mass fractions of 18C6 in methanol indicating that the ion-hydrophilic group interactions are stronger than the ion-hydrophobic group interactions. In the present ternary system interactions are taking place between the positive charge of ammonium groups and the alternative oxygen atom of the crown ether. The decreasing trend with increasing temperature suggests that the interactions between the drug molecule and crown molecules are decreased with increasing temperature. The facts support the data and the results observed from surface tension and conductivity study discussed earlier also support the facts.

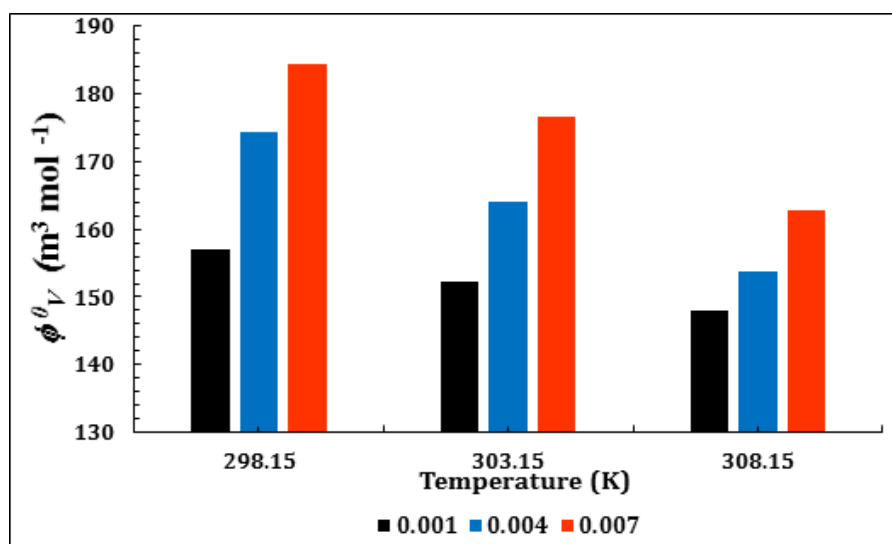


**Figure V.6:** Plot of limiting apparent molar volume ( $\phi_v^\circ$ ) of amantadine against different temperature (298.15 K, 303.15 K, 308.15 K) in mass fractions  $w_1=0.001$  (■),  $w_1=0.004$  (■),  $w_1=0.007$  (■) mass fractions of 18C6 in methanol solution.

The parameter  $S_V^*$  is the volumetric virial coefficient, and it characterizes the pair wise interaction of solute species in solution [50,51].  $S_V^*$  is found to be negative under investigations, which suggest that the pair wise interaction is restricted by the interaction of the charged functional group of ADH with crown. From **Table V.7**, a quantitative comparison between  $\phi_V^0$  and  $S_V^*$  values show that, the magnitude of  $\phi_V^0$  values is higher than  $S_V^*$ , suggesting that the solute-solvent interactions dominate over the solute-solute interactions in all solutions at the investigated temperatures.

### ***V.3.6. Temperature dependent limiting apparent molar volume:***

The variation of  $\phi_V^0$  with the temperature of the ADH in methanolic solution of 18C6 can be expressed by the general polynomial equation as follows,

$$\phi_V^0 = a_0 + a_1T + a_2T^2 \quad (6)$$

where  $a_0$ ,  $a_1$ ,  $a_2$  are the empirical coefficients depending on the solute, mass fraction ( $w_1$ ) of the co-solute Crown, and T is the temperature range under study in Kelvin.

The limiting apparent molar expansibilities,  $\phi_E^0$ , can be obtained by the following equation,

$$\phi_E^0 = \left( \delta\phi_V^0 / \delta T \right)_p = a_1 + 2a_2T \quad (7)$$

The limiting apparent molar expansibilities,  $\phi_E^0$ , change in magnitude of limiting apparent molar volume with the change of temperature. The values of  $\phi_E^0$  for different solutions of the studied ADH at 298.15, 303.15, and 308.15 K are reported in **Table V.8**. The table reveals that  $\phi_E^0$  is small negative in all studied temperature. This fact can ascribed to the presence of small caging or packing effect [52] for ADH in solutions.

**Table V.8:** Limiting apparent molar expansibilities ( $\phi_E^0$ ) for amantadine hydrochloride in different mass fraction of 18C6 in methanol solution ( $w_1$ ) at 298.15K to 308.15K respectively.

solvent mixture	$\phi_E^0 \cdot 10^6 (\text{m}^3 \cdot \text{mol}^{-1} \cdot \text{K}^{-1})$		
	Amandine + 18C6		
	298.15 K	303.15 K	308.15 K
$w_1 = 0.001$	-0.956	-0.880	-0.804
$w_1 = 0.004$	-2.095	-2.073	-2.051
$w_1 = 0.007$	-1.034	-2.170	-2.906

#### V.4. CONCLUSION

The present study shows that amantadine ion can bind nicely to three of the six available oxygen atoms in the 18C6 ring to form a stable complex (**Scheme V.2**) with 1:1 stoichiometry. The N-H...O hydrogen bridges between the ammonium functionalities and the oxygen acceptor heteroatoms of the crown ethers play a significant role in packing the host-guest complexes. The stable complex formation is established by physicochemical methods surface tension measurements, conductivity and IR study and the density data also support the interaction between amantadine ion and 18C6 systems. The inclusion complex formation has been explained qualitatively as well as quantitatively so as to make it dependable in its field of application.

The Host-guest complex formation based on the macrocyclic molecules is a facile and reversible process, which provides the feasibilities to design stimuli-responsive supramolecular systems and these macrocyclic molecules are basically friendly to the biological environment and exhibit good biocompatibilities. Crown ether-based host-guest interactions, which show good selectivity, high efficiency, and reversibility, have been structurally characterized and the underlying supramolecular chemistry has been presented in this work. Supramolecular chemistry i.e host-guest complex formation through noncovalent interactions offer the basis for novel approaches in medicine and also helps in understanding the interactions present in living systems. It was also found that host-guest complexation with crown ethers



resembles an established principle i.e. the hydrogen bonding acceptance as well as the donation propensity of crown ethers.

Amantadine is an antiviral agent that specifically inhibits influenza A virus replication at micromolar concentration. This drug is also very effective in the treatment of human Parkinson's disease. The host-guest complex is capable of protecting the drug molecule from chemical reactions and photochemical/thermal degradation in biological environment and the encapsulated drug can also be released sustainably from the cavity of macrocyclic molecule, achieving prolonged therapeutic effect.